East West University

Study of Ultrasound Based Imaging System for Cancer Detection

by

Sazib Paul	(SID: 2007-2-80-006)
Sudeep Banik	(SID: 2007-2-80-038)
A.B.M Shariful Arefin	(SID: 2007-2-80-039)

A thesis submitted to the Department of Electrical and Electronic Engineering

of

East West University

In partial fulfillment of the requirement for the degree of

Bachelor of Science in Electrical and Electronic Engineering

Summer 2011

14.09.2011

_____

Academic Supervisor

Dr. Mohammad Ariful Haque

14.09.2011

Department Chairperson

Dr. Anisul Haque

Abstract

Before the advent of medical imaging, palpation was one of the main methods to detect abnormalities in the body, mainly because the mechanical properties of diseased tissue are typically different than that of the healthy tissue surrounding it. Utilizing the same concept of palpation now ultrasound elasticity imaging technique is a promising new tool for cancer diagnosis and management. Ultrasound is applied to sense small local tissue deformations noninvasively to image stiffness and thus exploit the large intrinsic stiffness contrast generated during the progression of many diseases. Elasticity (strain) images are generally computed by measuring the local deformation due to the controlled application of static tissue compressive force. Local deformation is estimated by two techniques. One is correlation technique and another is compression technique. Correlation based strain imaging is efficient in cancer detection for its simplicity and lower cost but large displacement estimation error occurs in this technique. Therefore, in our thesis we investigate direct compression technique for strain imaging that provide significantly better image for cancer detection. But compression technique has a limitation in cancer detection which is computational cost. Computational cost is higher in compression technique. To overcome this limitation we apply frame wise compression technique which made the algorithm faster. In our work, we construct an elasticity image from the radio frequency ultrasound signals acquired before and after applying a physical pressure in the region of interest. We observe that, normal B-mode image cannot detect the cancer or hard tissue surrounding by normal tissue. On the other hand, strain image can detect cancer or hard tissue surrounding by normal tissue. For this reason people are trying to incorporate strain imaging technique in ultrasound equipment commercially. Therefore strain/elasticity imaging is now showing potential in early cancer detection.

Dedication

To our beloved parents.

ii

Acknowledgements

At first we would like to convey our cordial thanks and express our heartfelt gratitude to Almighty God to complete our thesis successfully. Without HIS assistance we could not have completed our thesis successfully.

We would like to express our gratitude to our honorable supervisor, Dr. Mohammad Ariful Haque, Assistant Professor, Department of Electrical and Electronic Engineering, Bangladesh University of Engineering and Technology (BUET), Dhaka, for his constant guidance and support in our thesis. He bestowed us with his invaluable suggestion and boundless inspiration throughout of this thesis work.

We would also like to thank Professor Dr. Anisul Haque, Chairperson, Department of Electrical and Electronic Engineering, East West University (EWU), Dhaka, for his support throughout our academic life. We are also grateful to all of our teachers and friends for their cooperation and encouragement throughout our whole academic life in EWU.

We would also like to express our acknowledgement and heartfelt gratitude to our beloved parents who have always been the true support and conferred us with their endless affection. We humbly dedicate this thesis to them.

Approval

The thesis titled "Study of Ultrasound Based Imaging System for Cancer Detection" submitted by Sazib Paul (ID: 2007-2-80-006), Sudeep Banik (ID: 2007-2-80-038), A.B.M Shariful Arefin (ID: 2007-2-80-039), session summer 2011, has been accepted satisfactory in partial fulfillment of the requirement of the degree of Bachelor of Science in Electrical and Electronic engineering on August 2011.

14.09.2011   (Supervisor)

Dr. Mohammad Ariful Haque

Assistant Professor

Department of Electrical and Electronic Engineering

Bangladesh University of Engineering and Technology (BUET), Dhaka.

14.09.2011   (Chairperson)

Dr. Anisul Haque

Professor

Department of Electrical and Electronic Engineering

East West University (EWU), Dhaka.

Declaration

We hereby declare that we are the sole authors of this thesis and it has not been submitted elsewhere for the award of any degree or diploma. We authorize East West University to lend this thesis to other institutions or individual on request for the purpose of scholarly research only.

We further authorize East West University to reproduce this thesis by photocopy or other means in total or in part at the request of other institutions or individuals for the purpose of scholarly research only.

Countersigned

Signature of Students

14.09.2011

15-09-11

Dr. Mohammad Ariful Haque

Sazib Paul

Assistant Professor

14/09/2011

Department of EEE

BUET

Sudeep Banik

(Thesis Supervisor)

S. Arefin
14.09.2011

A.B.M Shariful Arefin

Contents

Chapter-01   Introduction

Chapter-02   Literature Review

List of Figures

ix

Chapter 1

Introduction

1.1 Motivation

According to the American Cancer Society, more than 1.3 million new cases of cancer will be diagnosed, and more than half a million are expected to die of cancer - more than 1,500 people a day [1]. Every week around 10,000 people die of cancer which show the death rate for cancer deaths can't change in the last 10 years [2]. As there is no recovery from cancer perfectly, so early stage detection can provide trends to successful prevention. Chemo therapy and radiation therapy only save around 10% of the people treated and other treatment contribute little bit. On the other hand if cancer is not detected at early stage the abnormal cell from which cancer starts divides into two abnormal cells, then four cells, and so forth means cancer spread throughout the body and cases early death. Since the early beginnings of medical practice, the estimation of tissue hardness has been practiced through palpation, i.e. the act of feeling or pushing on various parts of a patient's body to determine medical conditions. Palpation has been an important tool to detect abnormalities in the body, mainly because the mechanical properties of diseased tissue are typically different than that of the healthy tissue surrounding it. A tumor or a suspicious cancerous growth is normally much stiffer than the background of normal soft tissue [3]. The basic relationship between tissue elasticity and hardness to palpability then follows the relationship that in order to be palpable, the object must be harder than the tissue surrounding it. However in many cases despite the differences in stiffness, the small size of a pathological lesion makes it harder to detect, and lesions located at deeper depths than the fingers are able to sense preclude its detection and characterization. Palpation is then limited to the detection of abnormalities and tumors which are close to the skin. If cancer is occurs not close to skin surface that means cancer is occurs depth in the body such as occurs in the lever, kidney, lung etc then manual palpation can to detect the position of the cancer. In addition, other properties have been

1

associated with diseased tissue, such as water content, acoustic tissue scattering and tissue density, giving rise to the field of medical imaging that allows imaging diagnosis well beyond the limits of palpation. Medical imaging systems such as computed tomography (CT), magnetic resonance imaging (MRI), and ultrasound, are widely used for early detection of cancer. However, despite the great and ongoing progress in medical imaging, it is recognized that only a small percentage of cancers can be diagnosed through noninvasive screening. But the detection of cancer is difficult in some cases and also the cost related to detection of cancer is expensive. On the other hand ultrasound based imaging is a simple test to detect cancer tissue and it is an inexpensive test that doesn't cause any discomfort or anxiety. Ultrasound tests also don't emit any radiation, so this technique is safe for everyone. Ordinary ultrasound has the advantage of imaging deep inside the body, but is virtually unable to differ between tissue of various hardness and elasticity, and there has been a consistent interest in tissue hardness, motion and vibration over the years. Tissue elasticity is characterized by the amount of tissue displacement or distortion in response to the application of an external force. Elasticity imaging is a method to remotely estimate elastic properties of biological tissues. Elasticity imaging has for instance been reported to be useful for the diagnosis and characterization of various tumors, which are usually stiffer than normal tissue. For example, tumors of the prostate or the breast may be invisible or barely visible in standard ultrasound examinations, yet are much stiffer than the surrounding tissue. So in our thesis we choose ultrasound based elasticity imaging technique because by improving its problem to serve the people to detect cancer at less cost and quickly.

1.2 Prospect of cancer detection using ultrasound based elasticity imaging techniques

Cancer is a class of diseases in which a group of cells display uncontrolled growth, invasion that intrudes upon and destroys adjacent tissues, and sometimes metastasis, or spreading to other locations in the body via lymph or blood. So, Cancer is the uncontrolled growth of abnormal cells in the body. Cancerous cells are also called malignant cells. Cancer grows out of normal cells in the body. Normal cells multiply when the body needs them, and die when the body doesn't need them. Cancer appears to occur when the growth of cells in the body is out of control and cells divide too quickly. Only early detection of cancer improves the trend of successful

treatment and survival. Physicians use information from symptoms and several other procedures to diagnose cancer. There are various imaging techniques to detect the cancer. One of these techniques is ultrasound imaging technique. Ultrasound imaging, also called sonography is a real-time and relatively inexpensive modality that is widely used in the purpose of clinical practice. Ultrasound is excellent for non-invasive imaging and diagnosis of various tissue abnormalities. There are, however, some limitations of ultrasound imaging. Perhaps the most important one is the ability of ultrasound imaging to identify all abnormalities - there may be low or no contrast between the abnormality and the surrounding tissue in ultrasound images [4].In case of cancer changes occurs in the mechanical properties of the tissues. Normal ultrasound imaging can't detect the change of mechanical properties (hardness or stiffness properties) of cancer tissues. So, come out from these types of failure of normal ultrasound we choose the ultrasound based elasticity imaging technique. Elasticity imaging is a new approach to medical imaging. Elasticity imaging, sometimes referred to as "mechanical imaging," is a non-invasive analysis of tissue movement and displacement so, it is the non-invasive imaging methods based on the mechanical response of an object to a vibration or impulsive force. Tissue displacement occurs anytime body tissue moves in response to pressure. As areas of abnormal tissue form within an organ, the tissue often becomes denser and less elastic. When pressure is applied to the organ, abnormal tissue and /or cancer cell generally exhibits less displacement than normal tissue. Ultrasound elasticity imaging is such a technique that emulates palpation. According to this technique, an ultrasound transducer is used as a remote sensing device to scan an object within a region of interest (ROI) both before and after compression is applied. The 2-D displacement function is then estimated by comparing the pre- and post-compression scans. From the estimated displacement function object strain and/or elastic constants can then be estimated. There are different techniques to detect the cancer using ultrasound based elasticity imaging. Among these techniques two common techniques are correlation technique and compression or stressor technique. But compression or stressor technique is better than the correlation technique, because correlation technique doesn't perfectly detect the hardness properties of cancer cell and disadvantage using cross-correlation techniques include the sensitivity of cross-correlations to amplitude variations in the presence of small signal distortions. So we chose the compression technique to detect the cancer using ultrasound based elasticity imaging.

1.3 Principles of elasticity imaging:

The elasticity imaging method is based on external tissue compression, with subsequent computation of the strain profile along the transducer axis. In ultrasound elasticity imaging system two different sets of RF data from the same region of interest (ROI) are collected and stored. First a conventional scan is made, then the tissue is compressed slightly, and another set of RF signals is collected. Two frames of ultrasound data are then recorded, one before and one after a section of tissue is uniform compressed by a small amount (e.g. with the ultrasound transducer).

(a)   (b)
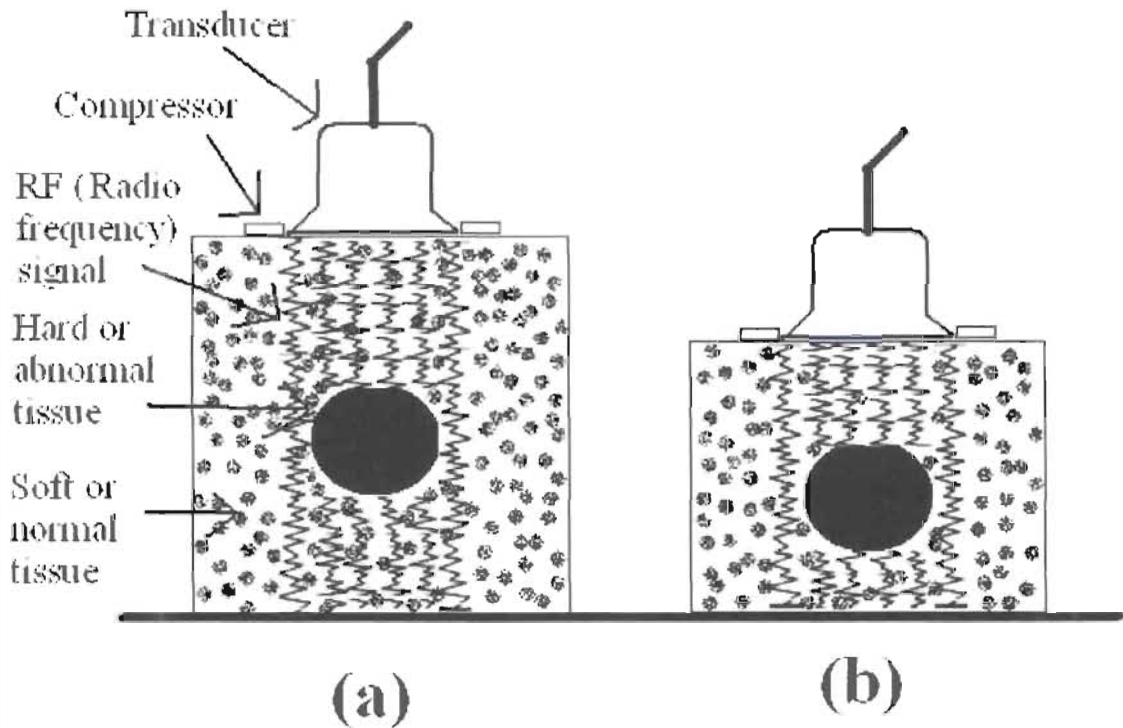
Figure1.1: The principle of ultrasound elasticity imaging. (a) Before compression ultrasound RF data and (b) after uniform compression ultrasound RF data.

Figure 1.1 shows the general concept behind elastography by showing the example of an applied compression used to detect a harder lump embedded in a softer medium. From the figure1.1 see

4

that hard or abnormal tissue is less compressed than soft or normal tissue. That means abnormal tissue is harder than normal tissue surrounding them. It is the main point of view in elasticity imaging system and establishes the relationship between these before and after compression data.
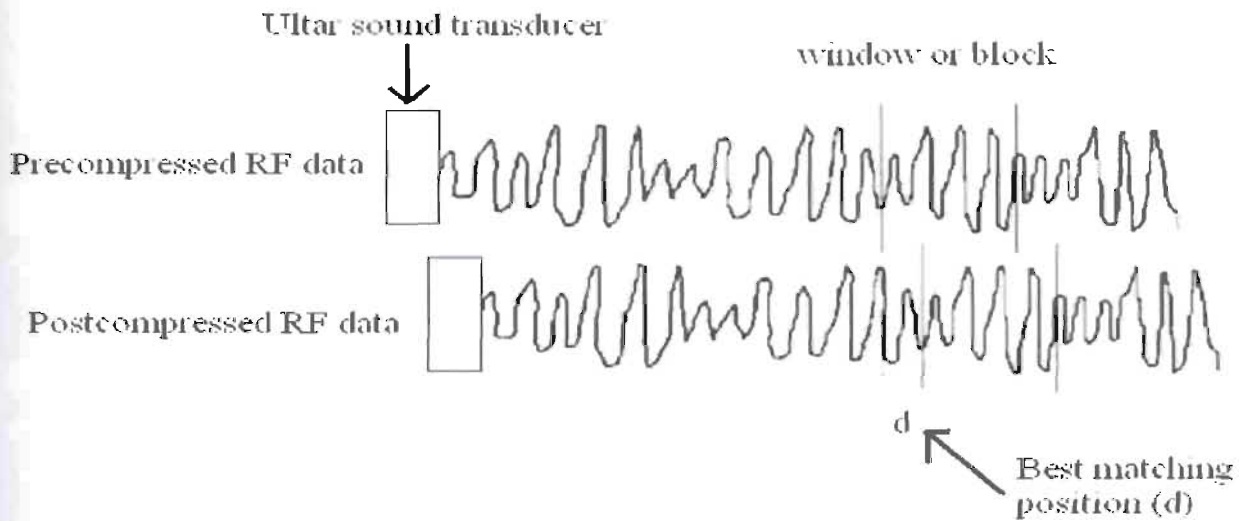
Figure1.2: Matching the pre-compressed and post-compressed data.

In elasticity imaging system, the post-compression RF signal or RF data is considered to be a compressed and shifted version of the pre-compression RF signal or RF data:

$$X_2(t) = X_1(a \cdot t + t_0) \dots\dots\dots\dots\dots\dots\dots\dots\dots\dots\dots\dots (1.1)$$

Where, $X_1(t)$ = pre-compression signal, $X_2(t)$ = post-compression signal, a= amount of compression and t_0= amount of shift.

The strain is derived by analysis of pre-compression and post-compression profile of the axial amount of compression and shift along the RF signal, and several techniques are available for estimating the amount of shift and amount of compression in tissues. The resulting tissue amount of shift and amount of compression between the two sets of RF data is usually tracked by different techniques. For estimating the tissue displacement a window or block around the sample range is used to improve the estimate. And find similarity within the sample window or block between a frame before and after pressure is applied. That means find how much the

signal, i.e. the tissue, has shifted or compressed for that range in the image as shown in figure1.2. To observe the similarity or matching between these two data several techniques is used. In these techniques, the amount of shift and amount of compression between two RF signals, x1(t) and x2(t) is found by searching the maximum matching position as also show in figure1.2. And also display the amount of shift and amount of compression image (resulting strain image). This resulting strain image is called elasticity image.

1.4 Proposed techniques for cancer detection

In this thesis we concentrate on the elasticity imaging, that employ the compression on the tissue surface. There are several techniques are used to detect the cancer tissue or hard tissue using ultrasound based elasticity imaging such as Vibration Amplitude Imaging, Compression Strain Studies, Multiple-step Compression-strain Sonoelastography, Tissue Motion with Speckle Tracking and sub-pixel registration method etc. From these techniques compression strain studies is easiest and simple method for detection of cancer. In previous sub-section we mention post-compressed signal is compression and shifted version of pre-compressed signal. So there are two procedures for detection of cancer using compression strain studies. One is observed the amount of shift and another is observer amount of compression. Amount of shift is observed by the cross-correlation technique. But in cross-correlation technique don't get the perfect matching position and for this reason get the undesired false peak. Another disadvantage of this technique is every point of pre-compressed signal is shifted for searching the maximum matching position. To improve this situation we observe the amount of compression by compression technique. In this technique two different sets of phantom RF ultrasound data from the same region of interest (ROI) are collected and stored by the ultra-sound transducer. Phantom means artificially made the tissue that contains cancer tissue or hard tissue. One data pre-compressed data and another data is post compressed data.
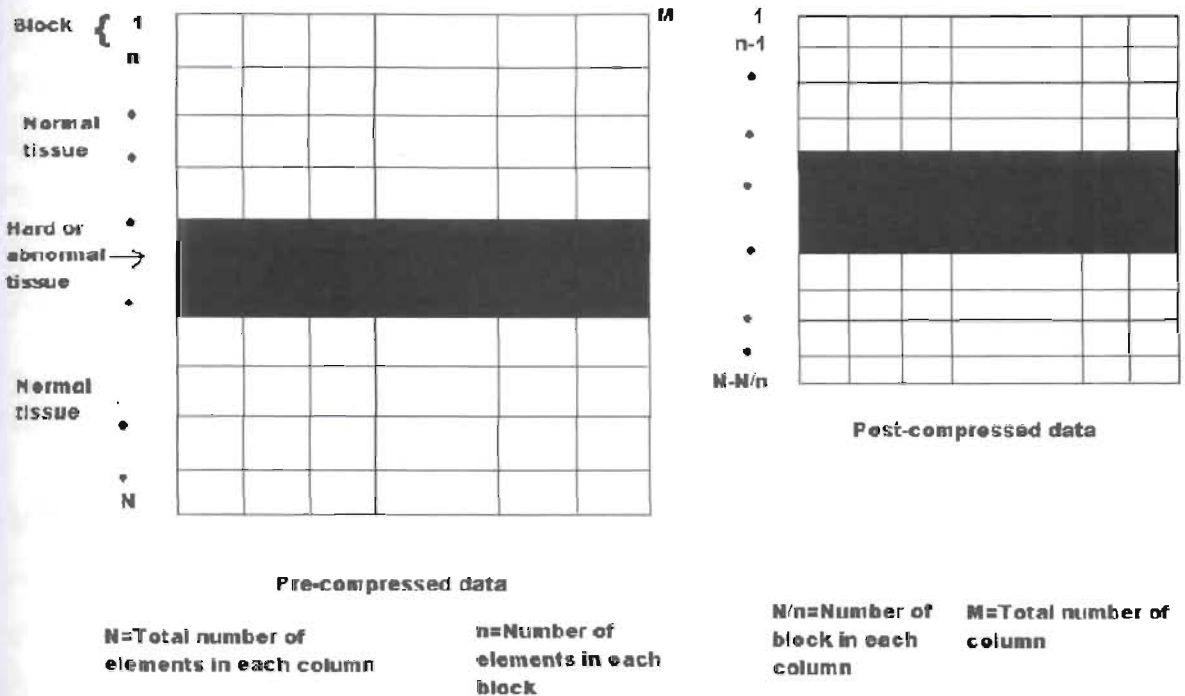
Figure1.3: Ultrasound phantom data show in block (pre-compressed and post-compressed).

Divide the pre-compressed and post-compressed data into some block as shown in figure1.3. Match the pre-compressed and post-compressed data using two compression techniques. 1st compression technique is artificially compressed the each block of pre-compressed data and matching with post-compressed data. 2nd compression technique is artificially compressed the frame of pre-compressed data and matching with compressed data. In both techniques we artificially compressed the pre-compressed data and matching with the post-compressed data than find out the best matching position.

1.4.1 Artificially block compression technique

This technique illustrates that, artificially compressed every block of the pre-compressed data and matched with post-compressed data. At first taking 1st block of pre-compressed data and the block is artificially not compressed then matching with the corresponding same size block of post-compressed data. In this method 1st, 2nd, 3rd times and so on artificially compressed the each block of pre-compressed data then matching with the corresponding same size block of the post-

compressed data. In all cases find the best matching position. When best matching position is find out then block of post-compressed data start from the best matching position. In this way all block of every row and every column in pre-compressed data is matching with the all same size block of every row and every column in post-compressed data. In this way find out the best matching position. In case abnormal or hard tissue we get the best match position for small amount of data displacement compare to normal tissue. This best matching position image is elasticity image.

1.4.2 Artificially frame compression technique

This technique illustrates that, artificially compressed the frame of pre-compressed data and matching with the post-compressed data. At first not we compressed the frame of pre-compressed data. Then we artificially compressed frame of pre-compressed data to assure that every block of pre-compressed data is compressed one times. Again artificially compressed frame of pre-compressed data to assure that every block is compressed two, three, four times and so on. Then taking uncompressed block from pre-compressed frame and matched with the corresponding same size block of post-compressed data frame. In this way taking the 1st, 2nd, 3rd .... times compression block of pre-compressed data frame and matched with the corresponding same size block of the post-compressed data frame. In all cases find the best matching position. When best matching position is find out then block of post-compressed data start from that position. In this way all block of every row and every column in pre-compressed data is matching with the all same size block of every row and every column in post-compressed data. In this way find out the best matching position. In case abnormal or hard tissue we get the best match position for small amount of data displacement compare to normal tissue. This best matching position image is elasticity image.

1.5 Organization of this thesis

This thesis consists of five chapters. Chapter 1 gives the motivation behind this thesis and the prospect of cancer detection using ultrasound based elasticity imaging techniques with the principle of elasticity imaging. This chapter also discusses about our proposed techniques for

cancer detection which are artificially block compression technique and artificially frame compression technique.

Chapter 2 is about the literature review of this thesis which consists of the basic principle about various techniques of elasticity imaging, which can be a method for detection of cancer and the existing methods for cancer detection.

In Chapter 3 we presents the detailed discussion of ultrasound imaging, which is a common diagnostic medical procedure to produce precise images of structures within the body such as the abdomen, breasts, female pelvis, prostate, scrotum, cardiology, obstetrics, cancer detection, thyroid and parathyroid glands, and the vascular system. This chapter also discusses about the basic block diagram of ultrasound imaging as well as the basic functionality of the ultrasound imaging. The different imaging modes of ultrasound imaging and the advantages and disadvantages of ultrasound imaging are also discussed in this chapter.

Chapter 4 is about our proposed technique for cancer detection. In this chapter we give a brief description about our proposed techniques which are artificially block compression technique and artificially frame compression technique. We developed the mathematical formulation for our proposed techniques and their corresponding results are also presented in this chapter.

Chapter 5 concludes the thesis by presenting the overall view of the thesis and pointing out some scope for future works for improving this thesis.

Chapter 2

Literature Review

2.1 Techniques for elasticity imaging

The concept of ultrasound based elastic imaging as discussed in previous chapter. For the detection of cancer tissue, various types of ultrasound based elastic imaging techniques have been developed by the extensive researches on this arena. In this chapter we review the different types of ultrasound based imaging techniques. These are Vibration Amplitude imaging, Compression Strain studies, Multiple-step Compression-strain Sonoelasticity, Transient elastography and tsissue motion with Speckle Tracking. Compression Strain studies contain the Combined Auto-Correlation (CAM) method, Normalized Cross-Correlation (NCC) method and Zero-Normalized Cross-Correlation (ZNCC) method. Multiple-step Compression-strain Sonoelasticity contain the Zero Phases Matching method.

2.2 Vibration Amplitude Imaging

Vibration amplitude sonoelastography detects a hard lesion by looking at the disturbance of the vibration amplitude pattern. Lerner and Parker first presented preliminary work on vibration amplitude sonoelastography ("sonoelasticity imaging") in 1987 [5]. In general, the lowest frequency modes are preferred because the lowest frequency is the easiest to excite and to interpret. In this method, a low frequency vibration (20-1000 Hz) is applied externally, and is transmitted in the tissue of interest. A hard inhomogeneity covered by soft tissue induces a disturbance in the normal vibration eigenmode patterns. Color Doppler imaging is then used to detect the resulting tissue stiffness. Since the velocity of propagation is a function of the elastic properties of tissue, measurement of the velocity of a propagating mechanical vibration in tissue will yield the differences in elasticity. The concept is that stiff tissues will respond differently to an applied mechanical vibration than normal tissue. Areas, or tissue, of increased stiffness will

experience less or decreased vibrations which can be seen as a in the Doppler sonoelasticity image. The main advantage of this technique is the ability to view the in-vivo results in real time. In 1994, a mathematical model for vibration amplitude sonoelastography was completed [6]. A "sonoelastic Born" approximation was used to solve the wave equations in an inhomogeneous (but isotropic) medium. The total wave field inside the medium can be expressed as:

$$\Phi_{total}= \Phi_h+\Phi_s \dots\dots\dots\dots\dots\dots\dots\dots\dots\dots\dots\dots\dots\dots\dots (2.1)$$

Where, Φ_h is the homogeneous field or incident field. On the other hand Φ_s is the field scattered by the inhomogeneity.

2.3 Transient elastography

Transient elastography was presented by Sandir et.al. in 1999 [7]. The method relies on the observation on the propagation of a pulsed shear wave, i.e. a wave where the oscillations occurs perpendicular to the direction of energy transfer, to determine the elastic properties of tissue, also known as transient elastography. The shear wave has a very low-frequency (60 Hz), and the local velocity (typically from 1 to 10m/s). This wave propagating in the tissue and this wave is directly related to the Young's modulus, E. The Young's modulus is also known as the modulus of elasticity, and can be calculated by dividing the tensile stress by the tensile strain as given by this equation:

$$E= \frac{\text{tensile stress}}{\text{tensile strain}} = \frac{F/A0}{L/L0} = \frac{FL0}{A0L} \dots\dots\dots\dots\dots\dots\dots\dots\dots\dots (2.2)$$

Where E is the Young's modulus (modulus of elasticity), F is the force applied to the object, A_0 is the original cross-sectional area through which the force is applied, L is the amount by which the length of the object changes, and L_0 is the original length of the object.

2.4 Compression Strain Studies

The term "elastography" was developed by Ophir et. al. in 1991 as a quantitative method of imaging the elasticity of biological tissue by direct imaging of the strain and the Young's modulus of tissue [8]. This method is based on the static deformation of a linear, isotropic, elastic material. Externally compressed the tissue under inspection and used cross-correlation analysis on the pre and post-compression A-line pair. From these data, calculate the strain profile inside the tissue along the transducer axis. Also measured the stress field close to the transducer surface, and added corrections for the non-uniform stress field inside the tissue. Having both strain and stress fields, calculated the elastic modulus profile of the tissue, and displayed the information as an "elastogram." This elastogram also called elasticity image.

The first RF A-line is obtained with the transducer slightly pre-compressing the region of interest (ROI). The second RF A-line is obtained after axially compressing the region of interest (ROI) by dz (usually, dz is about 1% of the target length). The post-compression A-line is 2dz/c shorter than the pre-compression A-line, where c is the speed of the ultrasound in the region of interest (ROI). So the post-compression A-line is zero added to have the same length as the pre-compression data. Cross-correlation is applied between segments in an A-line pair.

The temporal location of the maximum peak of the cross-correlation function is the estimate of the time shift between the two segments. The time scale is relative to the face of the transducer, so the shift of the signal starts as zero at the beginning of A-line, and increases to 2dz/c at the end. If the elastic modulus differs somewhere along the line, little or no increase will show in the time shift of certain segments. After one A-line pair is processed, the corresponding strain profile was defined as a one-dimensional (I-D) graph showing the strain as a function of depth in the target. The quantity shown in the below Equation is a particular local estimate of the strain in the i-th depth increment:

$$s_i = \frac{t_{i+1} - t_i}{2dz\,/\,c} \quad \dots\dots\dots\dots\dots\dots\dots\dots\dots\dots\dots(2.3)$$

Where t_i is the time shift for segment i. After repeating the process for an array of all lines, obtained a strain image of the compressed target.

As the range of strain measurement starts from zero and increases, they choose to display the inverse of elastic modulus in the "elastogram" (stiffness), so that the display has a finite range. This technique may be used to detect tumors with increased stiffness inside compressible soft tissue. Compression strain studies not only used cross-correlation method it is also used combined auto-correlation method, normalized cross-correlation method, zero-normalized cross-correlation method for detection of cancer.

2.4.1 Combined Auto-Correlation method

The combined autocorrelation method, which produces an elasticity image with high-speed processing and accuracy, and achieves a wide dynamic range for strain estimation by combining two-step processing. In this technique, tissue compression as well as RF signal is used. Therefore, the RF signals before and after compression can be modeled as:

$$i_1(t,d) = A(t,d)\, e^{-j(\omega_o t - \theta)} \quad\quad\quad\quad\quad\quad\quad\quad (2.4)$$

$$i_2(t,d) = A(t-\tau, d-\mu_d)\, e^{-j[(\omega_o(t-\tau)-\theta]} \quad\quad\quad\quad (2.5)$$

where $i_1(t,d)$ and $i_2(t,d)$ are the complex RF signals measured before and after deformation respectively, $A(t,d)$ is the envelop, ω_o is the transducer's center angular frequency, τ is the time shift and μ_d is the lateral displacement. In this complex cross-correlation function is used.

Used the cross-correlation method first step is coarse estimation by searching maximum envelop correlation and the second step is a fine estimation by using the unwrapped phase which is obtained by first step.

2.4.2 Normalized Cross-Correlation method

In this technique, the echo signals before and after compressions are treated as complex signals shifted in time. If the echo signals before and after compression are x (n) and y (n) respectively then Normalized cross-correlation between them can be represented as follows:

13

$$C_{NCC}(i,j) = \sum_{i'=-M}^{M} \sum_{j'=-N}^{N} \frac{x_{m,n}(i,j) \cdot y_{m,n}(i+i',j+j')}{|x_{m,n}(i,j)| \cdot |y_{m,n}|} \quad \dots\dots\dots\dots\dots\dots (2.6)$$

where, $x_{m,n}(i,j) = x(m+i,n+j)$

$y_{m,n}(i,j) = y(m+i,n+j)$

$$|x_{m,n}| = \sqrt{\sum_{i=-M}^{M} \sum_{j=-N}^{N} [x_{m,n}(i,j)]^2} \quad \dots\dots\dots\dots\dots\dots\dots (2.7)$$

$$|y_{m,n}| = \sqrt{\sum_{i=-M}^{M} \sum_{j=-N}^{N} [y_{m,n}(i,j)]^2} \quad \dots\dots\dots\dots\dots\dots\dots (2.8)$$

Maximum phase angle is determined from the maximum value of C_{NCC}. Then time shift and displacement is determined from the maximum phase angle. Finally Differential strain is determined.

2.4.3 Zero-Normalized Cross-Correlation method

Zero normalized cross-correlation method implements the 2D based strain image. In Zero normalized cross-correlation method matching of the same points between the two images recorded before and after compression. If the windowed pre-compression signal is x (n) and the windowed post-compression signal is y (n), then ZNCC between them x (n) and y (n) is defined as follows:-

$$C_{ZNCC} = \sum_{i'=-M}^{M} \sum_{j'=-N}^{N} \frac{[x_{m,n}(i,j) - x_{m,n}][y_{m,n}(i+i',j+j') - y_{m,n}]}{\Delta x \times \Delta y} \quad \dots\dots\dots\dots (2.9)$$

Where,

$x_{m,n} = x (m+i,n+j)$

$y_{m,n} = y (m+i,n+j)$

$$[x_{m,n}] = \frac{1}{(2M+1)(2N+1)} \sqrt{\sum_{i'=-M}^{M} \sum_{j'=-N}^{N} [x_{m,n}(i,j)]^2}$$

$$[y_{m,n}] = \frac{1}{(2M+1)(2N+1)} \sqrt{\sum_{i'=-M}^{M} \sum_{j'=-N}^{N} [y_{m,n}(i,j)]^2}$$

14

$$\Delta x = \sqrt{\sum_{i=-M}^{M} \sum_{j=-N}^{N} \left[xm, n(i,j) - xm, n \right]2}$$

$$\Delta y = \sqrt{\sum_{i=-M}^{M} \sum_{j=-N}^{N} \left[ym, n(i,j) - ym, n \right]2}$$

The algorithm to construct the strain image is similar to the previous described with the normal cross correlation is replaced by zero-normalized cross correlation. Maximum phase angle is determined from the maximum value of C_{ZNCC}. Then time shift and displacement is determined from the maximum phase angle. Finally Differential strain is determined.

2.5 Multiple-step Compression-strain Sonoelastography

Compression strain sonoelastography was developed by a group at the University of Michigan, Ann Arbor, headed by O'Donnell [9, 10]. This method is given stiffness as a function of position, to predict the strain inside tissue given specific forces and boundary conditions. The technique, used to detect the strain inside the medium after deformation, is based on cross-correlation of ultrasound A-lines. The group suggested using large deformation to maximize the signal-to noise ratio (SNR) of the displacement and strain estimations. However, large displacement results in significant internal strain, which changes the spatial distribution of the scatterers within an area of the image, thus de-correlating the speckle patterns used for cross-correlation. Instead of this technique they used multiple small step deformations to produce a large total deformation. The total displacement was then calculated by accumulating the displacement between each small deformation. To determine the displacement inside the tissue after each small deformation they used baseband correlation. The time shift between the pre- and post deformation signals were estimated from the phase of their zero-lag correlation functions:

$$t_{BB} = \frac{\tan^{-1}\left[\operatorname{Im}(C'(0))/\operatorname{Re}(C'(0))\right]}{\omega 0} \quad\dots\dots\dots\dots\dots\dots\dots\dots\dots(2.10)$$

Where, $\tilde{C}$ is the baseband correlation function. Multiple-step compression sonoelasticity also used the zero phases matching method to determine the displacement. In this method, basic

concept is to calculate the local scaling factors and uses them adaptively to make the phase of the maximum of the correlation function zero or within some tolerance phase level.

The received echo signal can be modeled as:

$$x(t) = x(\alpha t) \dots\dots\dots\dots\dots\dots\dots\dots\dots (2.11)$$
$$y(t) = x(t + \alpha t - t) = x(t + t(\alpha - 1))$$
$$\text{or, } y(t) = x(t + \tau(t))$$

So, the scaling factor can be interpreted as a variable delay which depends on the position of interest (ROI).

Now, $\phi(\alpha')$ can be defined as the phase of the maximum of correlation between the pre-compression signal $x(n)$ and post-compression signal $y(n)$.

It can be noted that,

Case 01: When $\phi(\alpha') = $ positive then $y(n)$ is a stretched version of $x(n)$

Case 02: When $\phi(\alpha') = $ negative then $y(n)$ is a compressed version of $x(n)$

Case 03: When $\phi(\alpha') = $ zero then $y(n)$ is identical to $x(n)$

Thus iteratively α' is estimated and $y(n)$ is scaled with this factor and $\phi(\alpha')$ is calculated.

2.6 Tissue Motion with Speckle Tracking

2-D speckle tracking technique was developed by Trahey and his colleagues [11] to measure motion in soft tissue. The speckle tracking system employed a sum of absolute difference (SAD) method to estimate tissue motion in two dimensions. The echo data was first obtained for a 2-D "kernel" region of size $k(i\ j)$. At a later time, the data for a "search" region including and surrounding the kernel region was acquired: $s(i,j)$. The following equation was evaluated for each a and b until a minimum of $E(a,b)$ occurred:

$$E(a,b) = \sum_{i=1}^{m} \sum_{j=1}^{n} \{ k(i, j) - s(i - a, j + b) \} \dots\dots\dots\dots\dots\dots\dots (2.12)$$

Then, (a,b) was the movement of the "kernel" region between the time of the first and the second data acquisitions. Their system utilized three major components: an electromechanical vibrator to excite tissue motion, an ultrasound scanner that can output either RF or detected echo data, and a speckle tracking system for motion estimation. Synchronization was made between the three components so that phase information was preserved. The 2-D displacement information was displayed in real-time as 2-D map of colors.

Chapter 3

Overview of Ultrasound Imaging

3.1 Introduction

Ultrasound is one of the most widely used techniques in medical imaging. Ultrasound imaging is a common diagnostic medical procedure that uses high-frequency sound waves to produce precise images of structures within the body. Although this limit of frequencies varies from person to person, it is approximately 20 kilohertz (20,000 hertz) for healthy, young adults. As ultrasound images are captured in real-time, they can show the structure and movement of the body's internal organs, as well as blood flowing through blood vessels. Imaging by ultrasound has dramatically changed the investigation as well as management of many clinical problems of different parts in the body. Ultrasound (or sonogram) technology allows doctors to see inside a patient without resorting to surgery. Ultrasound imaging is often used to examine many parts of the body such as the abdomen, breasts, female pelvis, prostate, scrotum, cardiology, obstetrics, cancer detection, thyroid and parathyroid glands, and the vascular system. During pregnancy, ultrasounds are performed to evaluate the development of the fetus. The images produced during an ultrasound examination often provide valuable information in the field of diagnosing and treating a variety of diseases and conditions of the body. The popularity of ultrasound imaging arises because it provides high-resolution images and does not damage tissues with ionizing radiation. It is also mostly non-invasive, although an invasive technique like intra-vascular imaging is also possible. There are also novel non-imaging uses of ultrasound like bone densitometer where the ultrasound speed difference is used to measure the depth or width of bones non-invasively. Ultrasonic sound waves use in ultrasound imaging sends from a transducer at a frequency too high to be heard. The ultrasonic sound waves move through the skin and other body tissues to the organs and structures within the body at the time when the transducer is placed at certain locations and angles. The sound waves bounce off the organs like an echo and return to the transducer. The transducer picks up the reflected waves, which are then converted

by a computer into an electronic picture of the organs or tissues under study. The speed at which sound waves travel is affected by different types of body tissues. Sound travels quickly through bone tissue, and moves most slowly through air. The speed at which the sound waves are returned to the transducer, as well as how much of the sound wave returns, is translated by the transducer as different types of tissue. A clear conducting gel is placed between the transducer to eliminate air between the skin and the transducer for the best sound conduction and to allow the skin for smooth movement of the transducer over the skin. Normally ultrasound displays the images in thin, flat sections of the body. Current research in advancements in ultrasound technology includes three-dimensional (3-D) ultrasound that formats the sound wave data into 3-D images. Four-dimensional (4-D) ultrasound is 3-D ultrasound in motion.
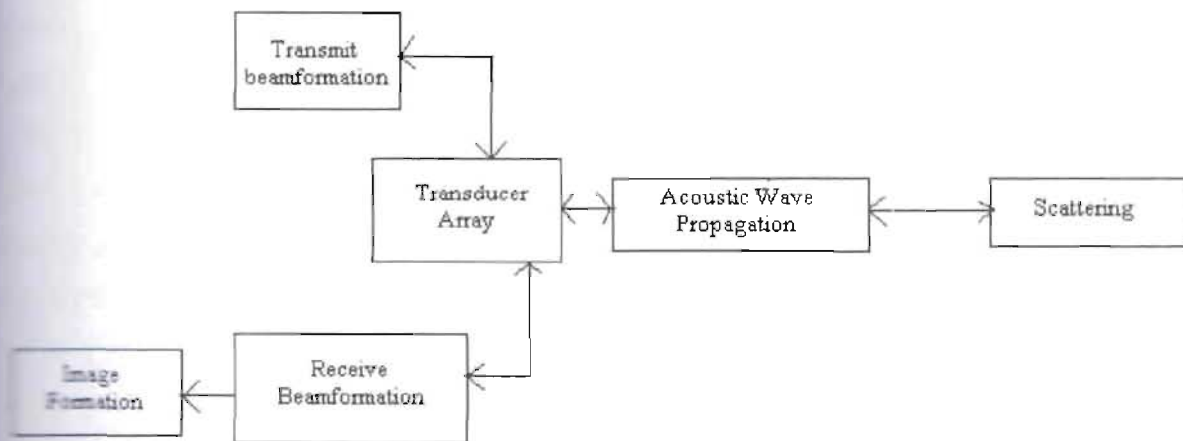
3.2 Working principle of Ultrasound Imaging

Figure3.1: Overall Block Diagram of an Ultrasound Scanner.

Ultrasonic imaging involves generation of acoustic wavelets, control of the timing and amplitude of these wavelets means to form beams and reception and processing of the echoes to form the image. Beam forming is a common signal processing technique used to create directional or spatial selectivity of signals sent to or received from an array of sensors or antennae. Generation of coordinated timing signals for transmit and delays for receive processes probably the most expensive building block is called beam formation. Transducers are usually multi-element arrays

19

piezoceramic elements. Image formation is conversion to video raster, image processing. The sequence of scanning starts with initiation of a scan by system processors. Beam former set to appropriate scan angle and transmit focal location. At the time of pulsing voltage applied to array elements followed by timed sequence sound emitted from elements and pre-amplifiers initiate reception of echoes. Receive beam former applies needed delays to optimize energy from desired focus and look angle and data stored and scan conversion to video raster begins and imaged formed. This process repeats itself.

3.3 Basic Functionality of ultrasound imaging

Basic ultrasound concepts that demonstrate how ultrasound systems works and how transducers focus sound waves along scan lines in the region of interest (ROI) discussed in this section. The frequencies that are referred for ultrasound system are greater than 20 kHz, which is commonly accepted to be the upper frequency limit the human ear can hear. Typically, ultrasound systems operate in the 2 MHz to 20 MHz frequency range, although some systems are approaching 40 MHz for harmonic imaging [12]. Basically the ultrasound system focuses sound waves along a given scan line so that the waves constructively add together at the desired focal point. The propagation of the sound wave towards the focal point is reflected from any object they encounter along their propagation path. Once all of the reflected waves have been measured with the transducers, the ultrasound system transmitted new sound waves towards a new focal point along the given scan line. Once all of the sound waves along the given scan line have been measured, a new scan line is focused from the ultra sound system until all of the scan lines in the desired region of interest have been measured.
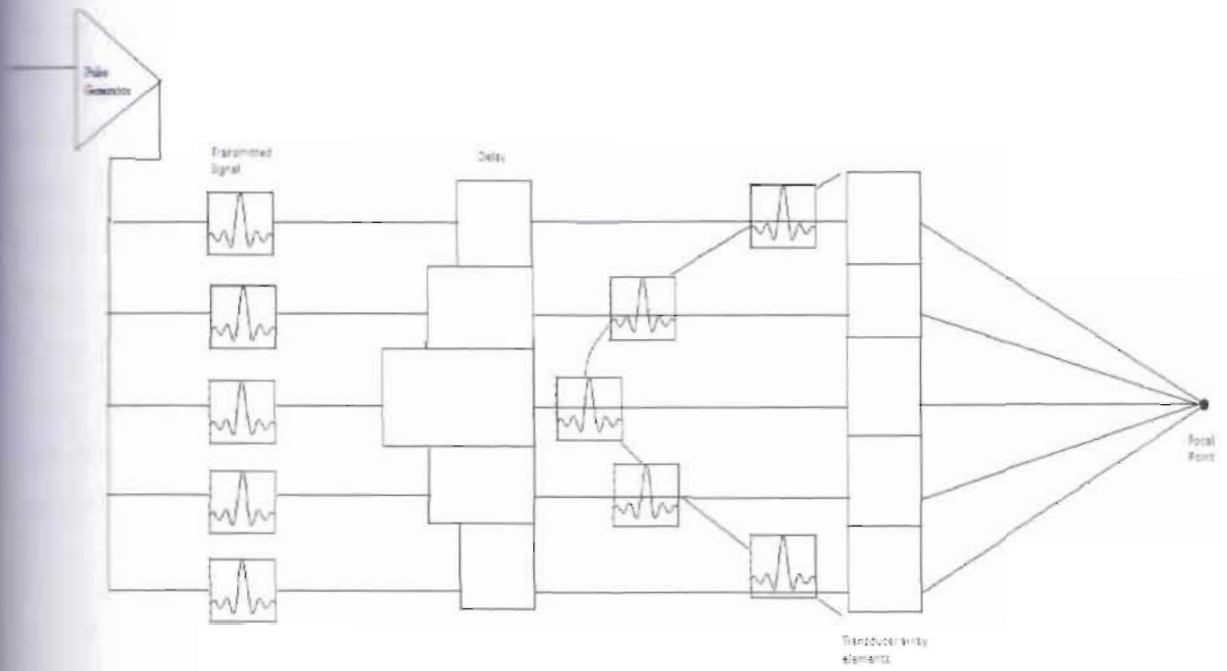
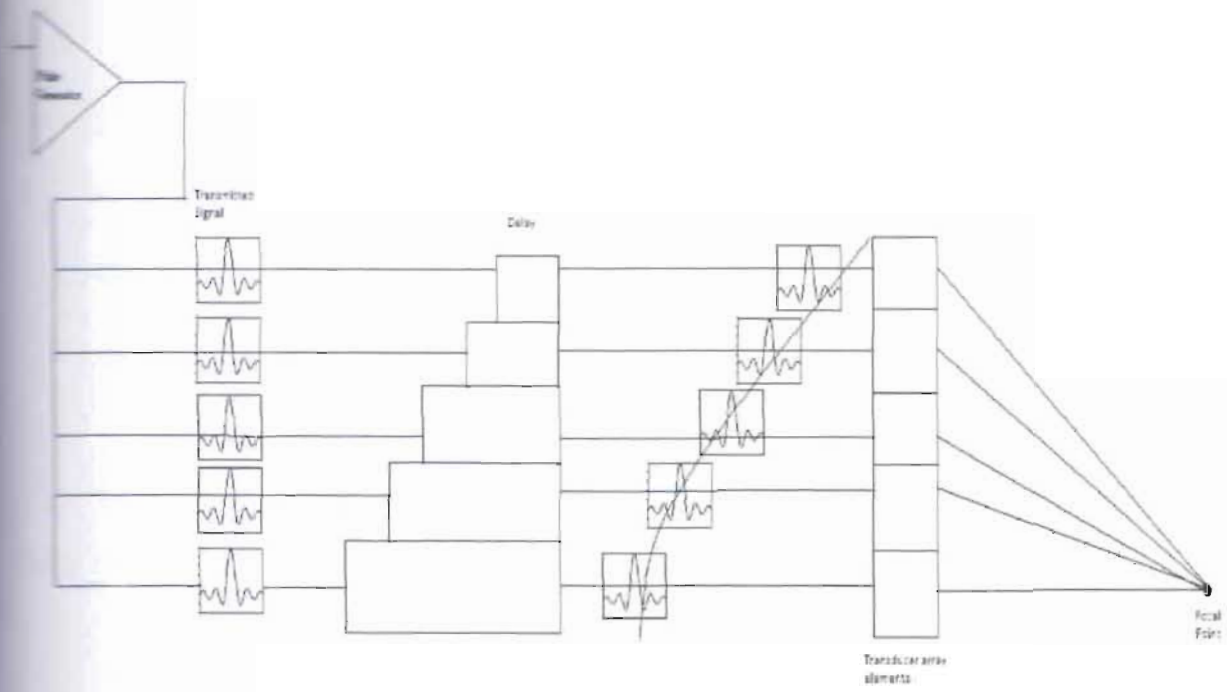**Figure3.2:** Transmit signal focusing in the region of interest.

Figure3.3: Transmit Signal steering and focusing in the region of interest.

21

In case of transmit focusing shown in figure1, the electrical signal coming from the pulse generator are delayed symmetrically using a delay line. The transducer which is near the focal point gets larger delay whereas the transducer which is far away from focal point gets smaller delay using the delay line. The delayed electrical pulses vibrates the transducer array producing sound waves that propagate through the region of interest (ROI) which is typically the desired organ and the surrounding tissue. As the transmit pulses are symmetrically delayed, they ultimately focus towards a particular focal point. The process of steering and focusing the sound beam in an ultrasound system is commonly referred to as phased array beamforming [13]. Transducers become sensors once transducers have generated their respective sound waves and can detect any reflected sound waves.
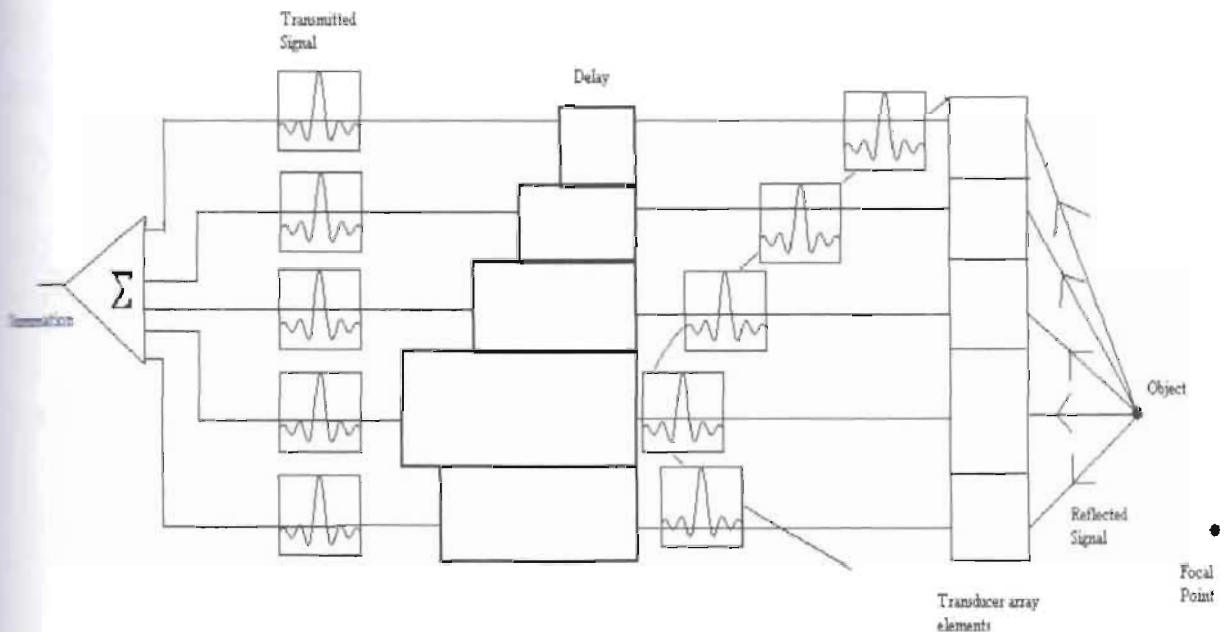

Figure3.4: Receive beamforming during signal acquisition from the region of interest.

When the transmitted sound waves encounter a change in tissue reflectivity within the region of interest, reflection occurs. The reflected sound waves are captured by each active transducer. The sound waves in each active transducer are asymmetrical delayed depending on the distance of desired focal point. The delay is asymmetrical because sound waves can reflect from any part of

22

region of interest if they encounter a change in tissue reflectivity. In ultrasound imaging, receive beamformer can be used to steer the beam by controlling the delay of each element. By controlling delay differences, dynamic focusing can be implemented on the receive beamformer side. These delay differences compensate for propagation delay differences between the focal point and the various elements of the array based on the array geometry. Assuming spherical reflected waves, these delay differences are bigger from targets in the near field where the wave front arriving at the array is more curved, and smaller from those in the far field where the arriving wave front is more flat. With dynamic focusing, these focusing delays (added to the steering delays) are not fixed, but rather are a function of time corresponding to the depth or range from which the echoes are being received during the scan-line The reflected sound waves from a longer distances compare to closer distances may be weaker or may be less reflectivity so, log compression technique is done to get the actual information. After passing through the delay line the sound waves are in parallel line and the peak of the received wave is detect by using envelope detection techniques and these parallel line sound waves are summed together. Once all of the amplitudes for all of the focal points have been detected, they can be displayed for analysis by the doctor or technician. Finally, for display on the CRT monitor a coordinate transformation called scan conversion need to be performed because ultrasound system usually operates, does not match the display coordinate system.

3.4 Imaging Modes

There are different types of imaging modes. Some are described below:

Amplitude mode: Amplitude mode or A-mode imaging as a function of time displays the amplitude of a sampled voltage signal for a single sound wave which is considered for 1-D. It is used to measure the distance between two objects by dividing the speed of sound by half of the measured time between the peaks in the A-mode plot, which represents the two objects in question. This mode is no longer used in ultrasound systems.

Brightness mode: Brightness mode or B-mode imaging is the same as A-mode, except that brightness is used to represent the amplitude of the sampled signal. It is used for producing a 2-D image.

Continuous Wave Doppler: Using Continuous Wave Doppler or CW Doppler, image can make. Procedure is a sound wave at a single frequency is continuously transmitted from one piezo-electric element and a second piezo-electric element is used to continuously record the reflected sound wave. By continuously recording the received signal, there is no aliasing in the received signal. Using this signal, the blood flow in veins can be estimated using the Doppler frequency. However, since the sensor is continuously receiving data from various depths, the velocity location cannot be determined.

Pulse Wave Doppler: In Pulse Wave Doppler or PW Doppler, along each scan line several pulses are transmitted. From the relative time between the received signals, the Doppler frequency is estimated as well as the velocity location can also be determined. A darker color usually denotes a larger magnitude while a lighter color denotes a smaller magnitude.

Color Doppler: In Color Doppler, the PW Doppler is used to create a color image that is super-imposed on top of B-mode image. A color code is used to denote the direction and magnitude of the flow. Red typically denoted flow towards the transducer and blue denotes flow away from it.

Power Doppler: In Power Doppler, instead of estimating the actual velocity of the motion, the strength or the power of the motion is estimated and displayed.

Harmonic Imaging: Harmonic Imaging is a new modality where due to the usual high frequency of the harmonic, these images have higher resolution than conventional imaging but due to higher loss, the depth of imaging is limited. This system imposes stringent linearity requirements on the signal chain components.

Elasticity Imaging: Elasticity or Strain Imaging is a new modality where some measures of elasticity of the tissue (usually under compression) is estimated and displayed as an image. This image is capable to distinguish between normal and malignant tissues. Both on clinical applications and in real-time system implementation Elasticity image is currently a very active area of research.

3.5 Advantages and Disadvantages of Ultrasound Imaging

The advantages of ultrasound imaging include bedside availability and the relative ease of performing repeated examinations. Imaging is real-time and free of harmful radiation. There are no documented side effects and discomfort is minimal. Despite the absence of randomized, controlled trials, ultrasound imaging guidance for interventional procedures in the thorax is likely to improve diagnostic yield and reduce complications by providing visual guidance [14]. It helps the physicians to decide whether is anything wrong within the body

The disadvantages of ultrasound imaging are primarily related to the fact that it is heavily operator-dependent. Retrospective review of images provides only limited quality control. In the obese patient ultrasound penetration may be limited so that deep structures may not be well seen. There is a trade-off in ultrasound between using the highest frequency probe possible to achieve high resolution and a lower frequency to achieve beam penetration. The ultrasound beam is also arrested by gas in the abdomen and is unable to penetrate bone

3.6 Conclusion

Modern ultrasound systems related to signal processing intensive. Better image quality and higher diagnostic value can be achieved by advanced techniques of signal processing. New advancements like 3D/4D imaging only increase the processing requirements of such systems. To add new functionalities into the systems are the challenges for the equipment manufacturers company.

Chapter 04

Elasticity imaging for cancer detection

4.1 Introduction

In this thesis, the objective is to detect cancerous tissue using ultrasound based imaging technique. Normal B-mode ultrasound image cannot differentiate between cancerous and non-cancerous tissue. Therefore we construct an elasticity image from the radio frequency ultrasound signals acquired before and after applying a physical pressure in the region of interest. In other words, elasticity imaging method is based on external tissue compression, with subsequent computation of the strain profile along the transducer axis. In this work, we used two different sets of real RF ultrasound data collected from the phantom subject. Phantom is an artificial tissue that contains hard object surrounded by soft gel-like material. We also acquired synthetic ultrasound data by running a MATLAB program for simulating ultrasound system. One set represents pre-compressed data and another set represents post compressed data. Collected data are displayed in B-mode image in figure01 and figure02. The first signal processing task for generating a strain image is estimation of local compression throughout the scan region. The inputs are pre-compressed and post-compressed signals of RF ultrasound data.
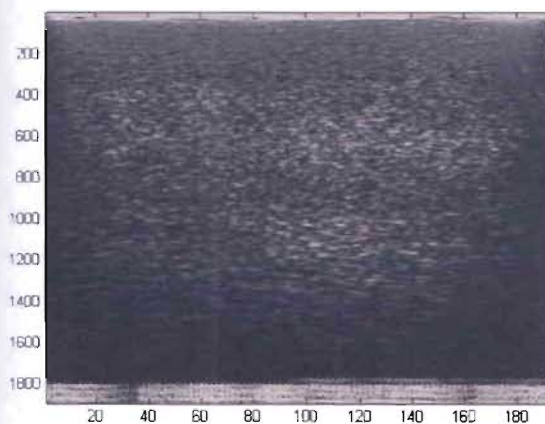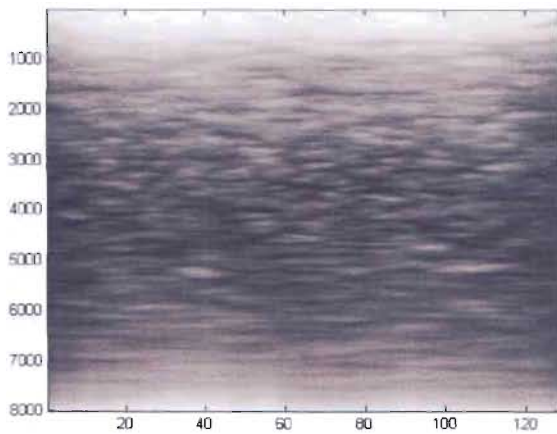

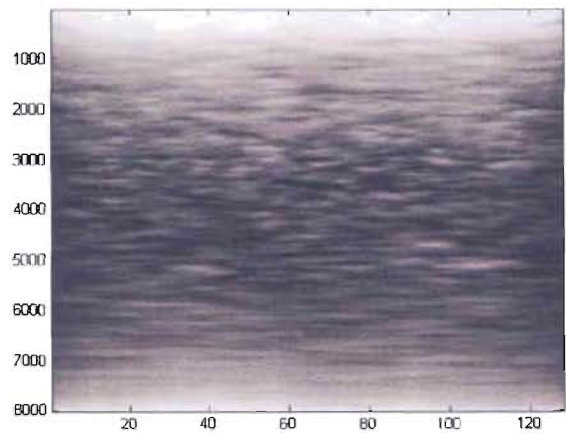Pre-compressed real ultrasound RF data from phantom subject
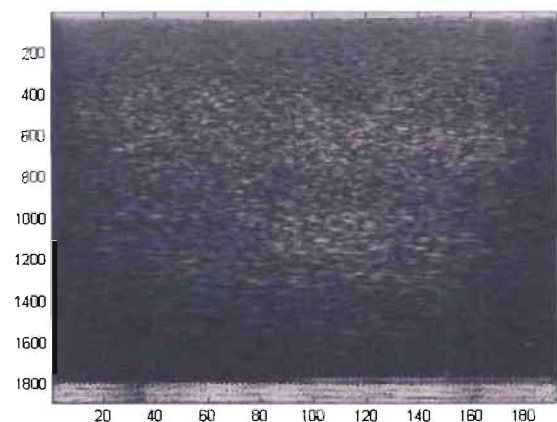
Post-compressed real ultrasound RF data from phantom subject

Figure4.1: B-mode imaging real ultrasound RF data from phantom subject.

Pre-compressed simulated data by using MAT-LAB

Post-compressed simulated data by using MAT-LAB

Figure4.2: B-mode imaging synthetic data by using MAT-LAB.

Normal B-mode imaging real ultrasound RF data and synthetic ultrasound data cannot detect the cancer or hard tissue surrounding by normal tissue. These types of imaging cannot differentiate between the normal tissue and cancer tissue. In figure4.1 and figure4.2 normal tissue and cancer tissue are look like same.

4.2 Mathematical Formulation

Two related scan-lines are collected from the ultrasound RF data. One scan-line is the pre-compressed signal which is collected from pre-compressed ultrasound RF data. Another scan-line is post compressed signal which is collected from post-compressed ultrasound RF data. The two scan-lines are shown in figure4.3 and figure4.4, respectively.

Let us consider,

Pre-compressed signal, $x_1 = s(t)$ (Shown in figure 4.3)

Post-compressed signal, $x_2 = s(at)$ (Shown in figure 4.4), compressed version of pre-compressed signal.

Where, a = amount of compression ('a' can be any value greater than one).

A block of data centered on the point of interest in the pre-compressed signal is compared with the post-compressed signal of equal size. A match is identified by calculating the similarity

27

between these two blocks, noting the post-compression block that registers the highest similarity. Finally, the displacement estimation is equal to the difference between the positions of the pre-compression and post-compression blocks. We used two methods for searching the best matching position or correct compression factor. One is block wise compression technique and another is frame wise compression technique. In these two techniques, we divide the pre-compressed and post-compressed data into a number of equal size blocks. In the first technique, we compress each block of pre-compressed signal using signal processing technique and then estimate the matching index with a block of post-compressed signal located in the related position. In the second technique, we compress the entire scan-line of the pre-compressed signal considering some pre-determined compression factors. Then we take every block of pre-compressed signal and match with the corresponding same size block of post-compressed signal. In both the techniques we observe the best matching position or correct compression factor from the maximum matching index for every block or window. Figure 4.5 show a typical matching index profile for a block or window where window size is 150 (shown in figure4.3 and figure4.4).
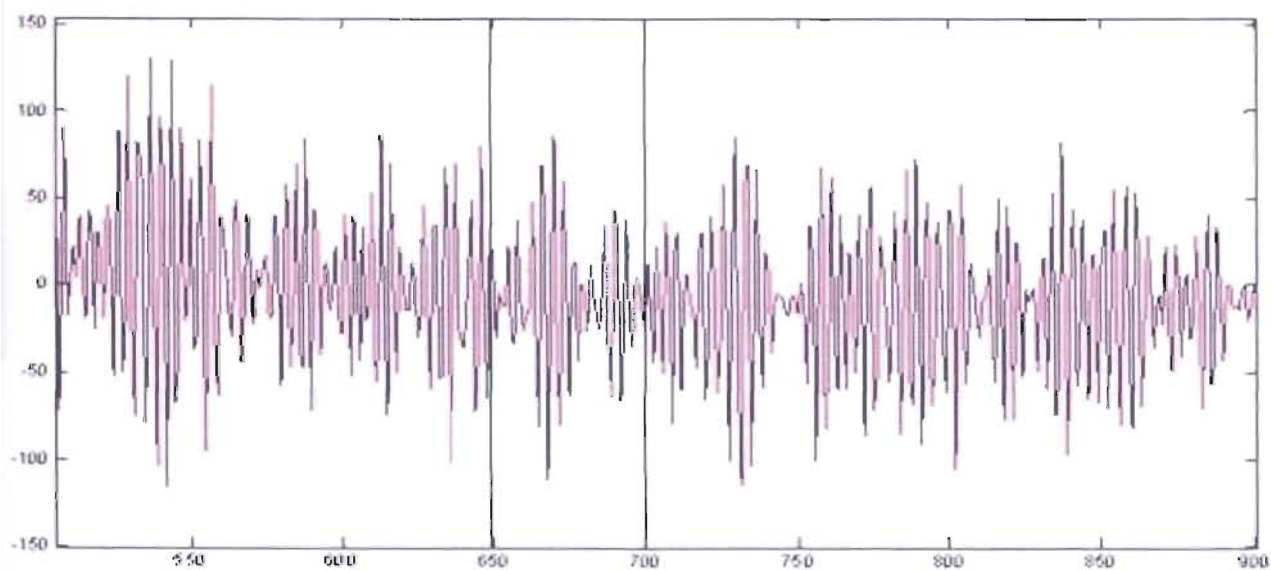

Pre-compressed signal window or block

Figure4.3: Pre-compressed signal.
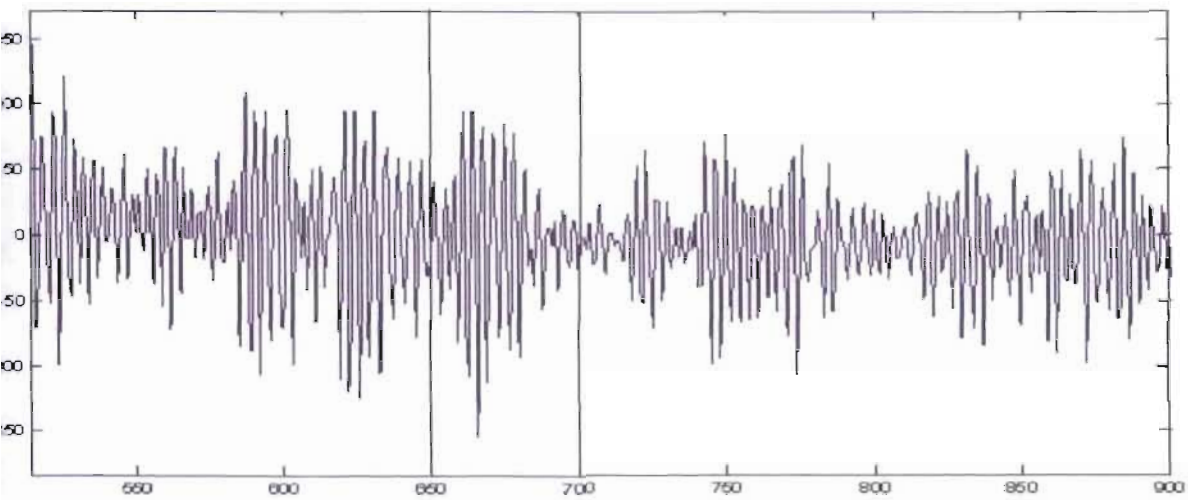
Post-compressed signal window
or block

Figure4.4: Post-compressed signal.

Maximum matching value

Correct compression factor or best
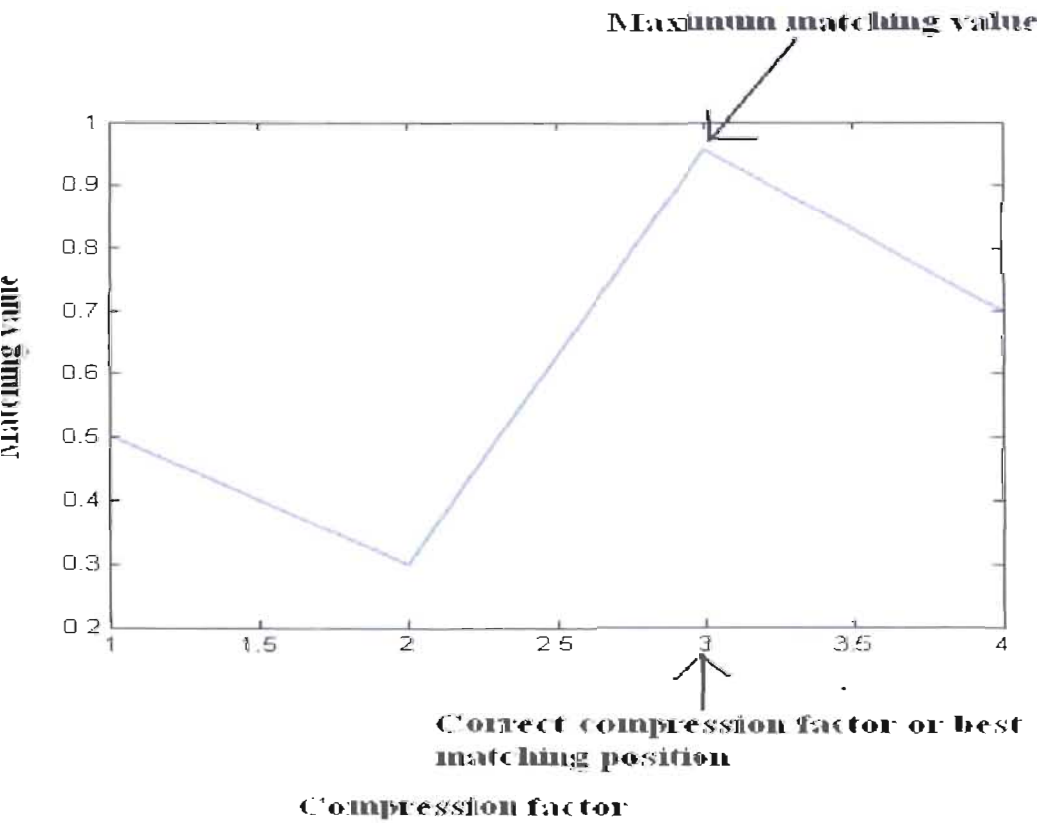matching position

Compression factor

Figure4.5: Highest matching value and corresponding compression factor or best matching
position.

29

.1 Block wise compression technique

this technique every scan-line of pre-compressed data and post-compressed data are divided o n blocks. We assume that each block or window of pre-compressed data and post-npressed data are equal size or length. Pre-compressed signal and post-compressed signal are pressed as $x^j_i(t)$.

here, i= 1 means pre-compressed signal and i= 2 means post-compressed signal

1,2,3,4,……………………,n-1,n means 1st, 2nd,3rd,4th……………………, n-1th,nth block pectively.

Pre-compressed signal
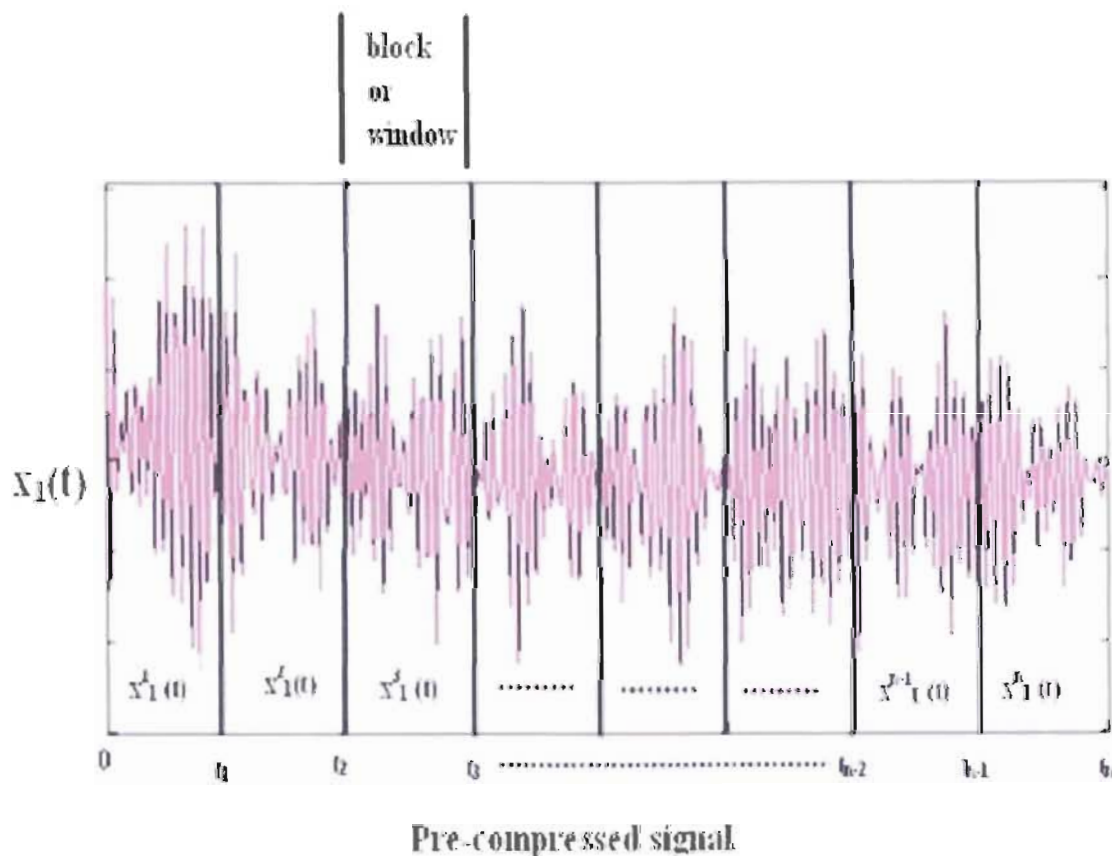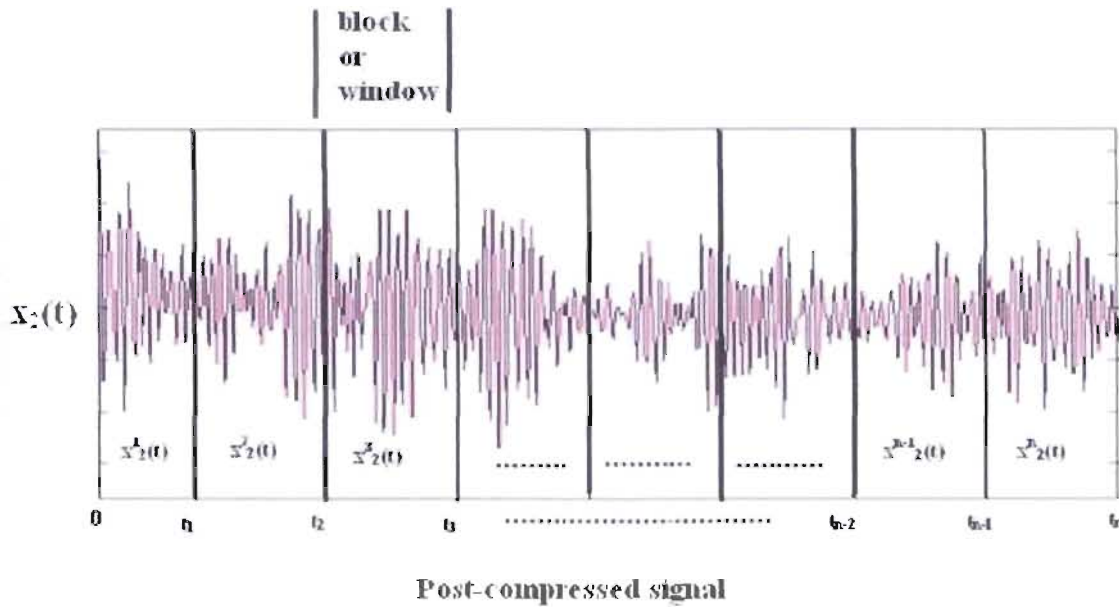
gure4.6: Pre-compressed signal $(x_1(t))$.

Figure4.7: Pre-compressed signal ($x_1(t)$).

First block of pre-compressed signal is expressed as $x^1_1(t)$ in the range $0<t<t_1$. First block of post-compressed signal is expressed as $x^1_2(t)$ in the range $0<t<t_1$. We compute the matching value between $x^1_1(t)$ and $x^1_2(t)$ using the index

$$\text{Matching index, } P_1 = \frac{\int_0^{t_1} x^1_1(\tau) x^1_2(\tau) d\tau}{\sqrt{\int_0^{t_1} |x^1_1(\tau)|^2 d\tau} \sqrt{\int_0^{t_1} |x^1_2(\tau)|^2 d\tau}} \quad \ldots\ldots\ldots\ldots\ldots (4.1)$$

Where, P_1 represents the normalized cross-correlation at zero lag between $x^1_1(t)$ and $x^1_2(t)$.

Now, we compress the First block of pre-compressed signal, $x^1_1(t)$, by a compression factor of 'a_1' using signal processing technique. In this work, we used 'resample' function of MATLAB that interpolates the compressed values by fitting with a tenth order polynomial function. The compressed signal can be expressed as $x^1_1(a_1 t)$ within the range $0<t< t_1/a_1$. Then we extract the corresponding same length block signal from the post-compressed signal which is expressed as $x^1_2(t)$ within the range $0<t<t_1/a_1$.

We compute the matching value between $x^1_1(a_1 t)$ and $x^1_2(t)$ using the same index

$$\text{Matching index, } P_2 = \frac{\int_0^{t_1} x^1_1(a_1\tau) x^1_2(\tau) d\tau}{\sqrt{\int_0^{t_1} |x^1_1(a_1\tau)|^2 d\tau} \sqrt{\int_0^{t_1} |x^1_2(\tau)|^2 d\tau}} \quad \ldots\ldots\ldots\ldots (4.2)$$

Where, P_2 represents the normalized cross-correlation at zero lag between $x^1_1(a_1 t)$ and $x^1_2(t)$.

31

Then, we compress the 1st block of pre-compressed signal ($x^1_1 (t)$) by a compression factor of 'a_2' which is expressed as $x^1_1 (a_2t)$ within the range $0<t< t_1/a_2$. [Note that $a_2> a_1$]

Then we extract the corresponding same length block signal from the post-compressed signal which is expressed as $x^1_2 (t)$ within the range $0<t<t_1/a_2$.

We compute the matching value between $x^1_1 (a_2t)$ and $x^1_2 (t)$ using the index

$$\text{Matching index, } P_3 = \frac{\int_0^{t1} x^1_1(a_2\tau)x^1_2(\tau)d\tau}{\sqrt{\int_0^{t1} |x^1_1(a_2\tau)|^2d\tau}\sqrt{\int_0^{t1} |x^1_2(\tau)|^2d\tau}} \quad \ldots\ldots\ldots\ldots\ldots (4.3)$$

The process continues for a compression factor of 'a_3', 'a_4', 'a_5', 'a_6' ,........, 'a_i'.

Now we find the best matching position observing the matching index profile. The maximum matching position, a_{max}, can be obtained by evaluating the following expression

$$a_{max} = \arg\max_{a_i} P_i \quad \ldots\ldots\ldots\ldots\ldots (4.4)$$

When the best matching position is obtained, the second block of post-compressed signal will start from that position. Second block of post-compressed signal is expressed as $x^2_2 (t)$ within range $t_1-a_i< t< (t_1-a_i+ t_1)$, where $t_2= t_1-a_i+ t_1$. Second block of pre-compressed signal is expressed as $x^2_1 (t)$, within range $t_1<t< (t_1+ t_1=2 t_1)$, where $t_2= t_1+ t_1=2 t_1$

We compute the matching value between $x^2_1 (t)$ and $x^2_2 (t)$ using the index

$$\text{Matching index, } P_1 = \frac{\int_{t1-ai}^{t2} x^2_1(\tau)x^2_2(\tau)d\tau}{\sqrt{\int_{t1}^{t2} |x^2_1(\tau)|^2d\tau}\sqrt{\int_{t1-ai}^{t2} |x^2_2(\tau)|^2d\tau}} \quad \ldots\ldots\ldots\ldots (4.5)$$

Where, P_1 represents the normalized cross-correlation at zero lag between $x^2_1 (t)$ and $x^2_2 (t)$. Now, we compress the First block of pre-compressed signal, $x^2_1 (t)$, by a compression factor of 'a_1' using signal processing technique. In this work, we used 'resample' function of MATLAB that interpolates the compressed values by fitting with a tenth order polynomial function. The compressed signal can be expressed as $x^2_1(a_1t)$ within the range $0<t< t_2/a_1$. Then we extract the corresponding same length block signal from the post-compressed signal which is expressed as $x^2_2 (t)$ within the range $0<t<t_2/a_1$.

The process continues for a compression factor of 'a_2', 'a_3', 'a_4', 'a_5',........, 'a_i' for pre-compressed signal.

32

Then we find the best matching position observing the matching index profile. The maximum matching position, a_{max}, can be obtained by evaluating the following expression

$$a_{max} = \arg\max_{a_i} P_i$$

.... (4.6)

When best matching position is obtain then third block of post-compressed signal will start from that position. Third block of post-compressed signal is expressed as $x^3_2(t)$ within range $t_2-a_i< t< (t_2-a_i+ t_2)$, where $t_3= t_2-a_i+ t_2$ Then we extract the third block signal from the pre-compressed signal which is expressed as $x^3_1(t)$ within range $t_2<t<(t_1+ t_1+ t_1=3 t_1)$, where, $t_3= t_1+ t_1+ t_1=3t_1$

In this way, we taken all blocks of all scan-line sequentially (fourth, fifth, ... ,n^{th}) and done same job.

4.2.2 Result of block wise compression technique

We obtain the amount of compression (a_i) from the maximum matching index for all blocks of all scan-lines. The amount of compression for all blocks of one scan-line is shown in figure4.8 and figure4.10 for real ultrasound data and synthetic data respectively. If hard tissue or cancer tissue is present then amount of compression factor is smaller compare to normal or soft tissue's compression factor. Because, for hard tissue maximum matching index is obtain by small amount of compression factor. But for normal or soft tissue amount of compression is larger compare to hard tissue also shown in figure4.8. Finally display the B-mode elasticity image (shown in figure4.9 and figure4.11). B-mode elasticity image contain the amount of compression for all blocks of all scan-lines.
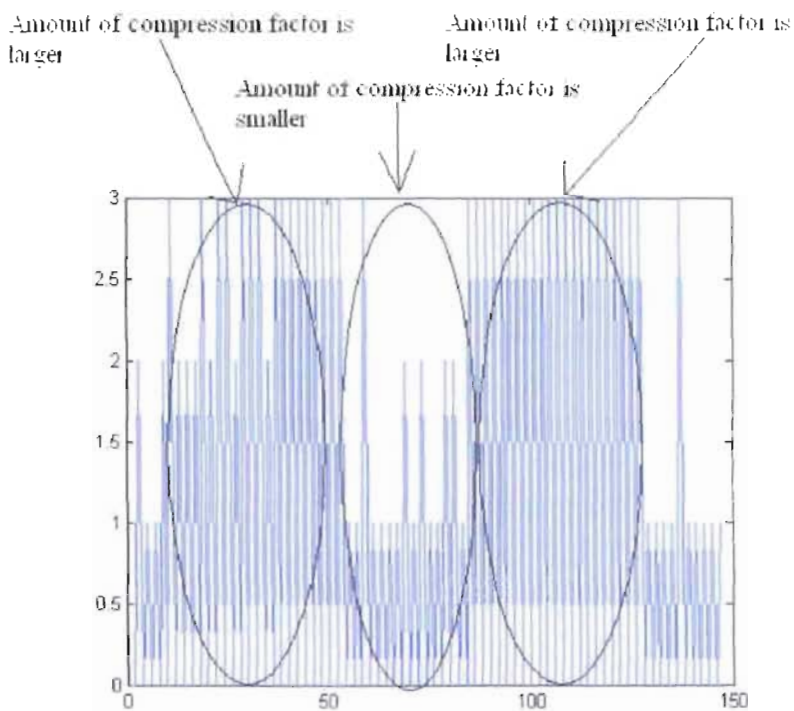
33

Figure4.8: Amount of compression for all blocks of one scan-line for real ultrasound data using block compression technique.
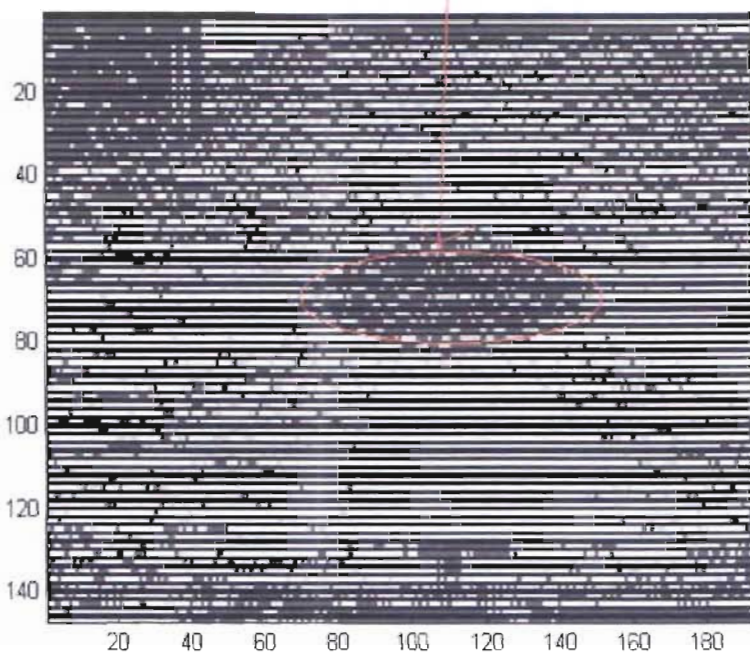
Hard tissue or cancer tissue

Figure4.9: B-mode elasticity image for real ultrasound data using block compression technique.
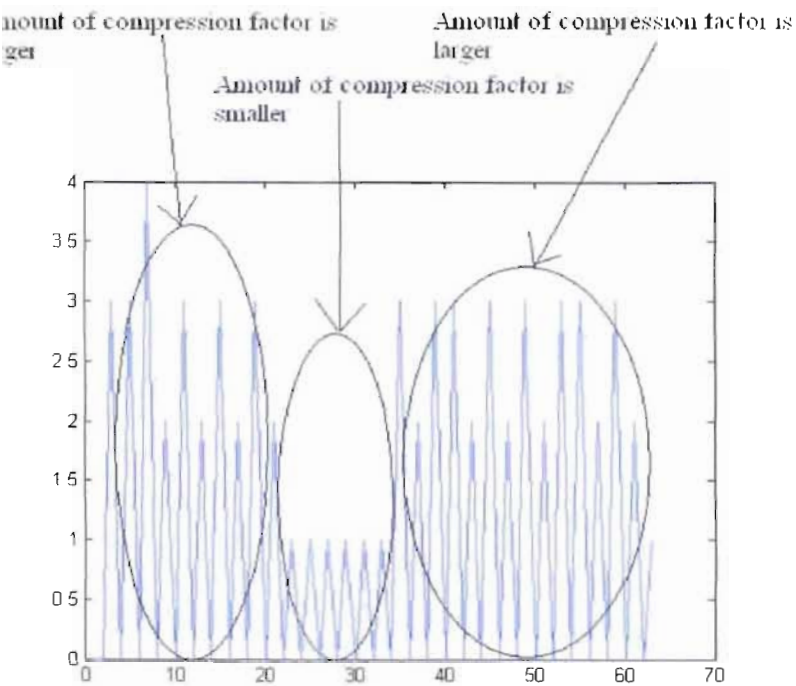
34

Figure4.10: Amount of compression for all blocks of one scan-line for synthetic data using block compression technique.
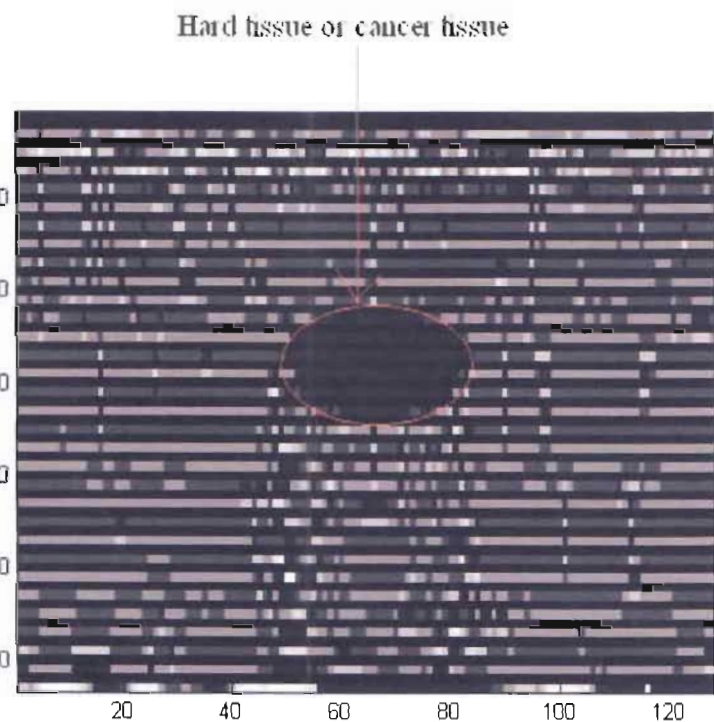

Figure4.11: B-mode elasticity image for synthetic data using block compression technique.

mode elasticity image is an amount of compression for all blocks of all scan-line. B-mode
sticity image detect the hard tissue or cancer tissue surrounding the normal tissue. In other
rd B-mode elasticity image differentiate between normal tissue and hard tissue. The cancer
sue is indicated by red color circle in B-mode elasticity image as shown in figure4.9 and
ure4.11 for real ultrasound data and synthetic data respectively. But in these B-mode images
veral noise are occurs in cancer tissue and surrounding normal tissue. And these images are
oking like so clumsy. There are unwanted peak is occurs in amount of compression image of
e scan-line (shown in figure4.8 and figure4.10). To overcome this situation we introduce
veral approaches later.

2.3 Frame compression technique

ock wise compression technique takes more time. So we introduce another technique. In this
chnique every scan-line of pre-compressed data and post-compressed data are divided into n
ock. We assume that each block of pre-compressed signal are equal size or lengths of the
ocks are same as shown in figure4.12. Also assume that, block size of post-compressed signal
e not equal as shown in figure4.12. This technique illustrates that, compressed the entire scan-
e of the pre-compressed signal considering some pre-determined compression factors and
atching with the post-compressed signal. At first we uncompressed the entire scan-line of pre-
mpressed signal and matching with the corresponding same size block of post-compressed
gnal as shown in figure4.12. Then we compressed the entire scan-line of pre-compressed signal
compression factors 'a_1' and matching with the corresponding same size block of post-
mpressed signal as shown in figure4.13. In this way we compressed the entire scan-line of pre-
mpressed signal by compression factor 'a_2' and matching with the corresponding same size
ock of post-compressed signal as shown in figure4.14. Note that, 'a_2' is greater then 'a_1'. The
ocess continues for a compression factor of 'a_3', 'a_4', 'a_5', 'a_6' ,........, 'a_i'.
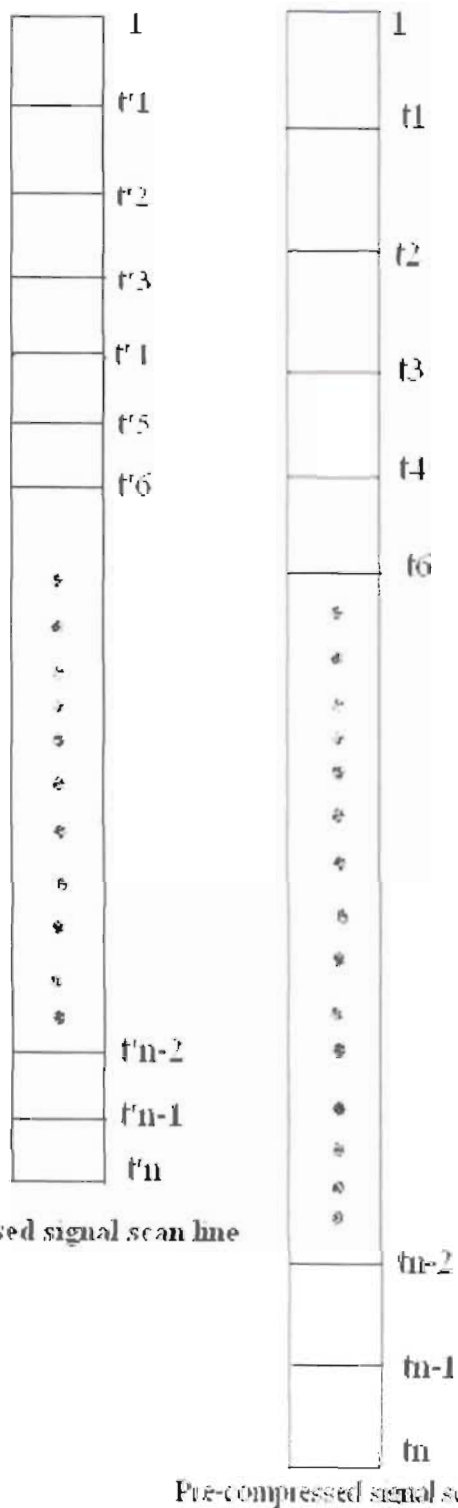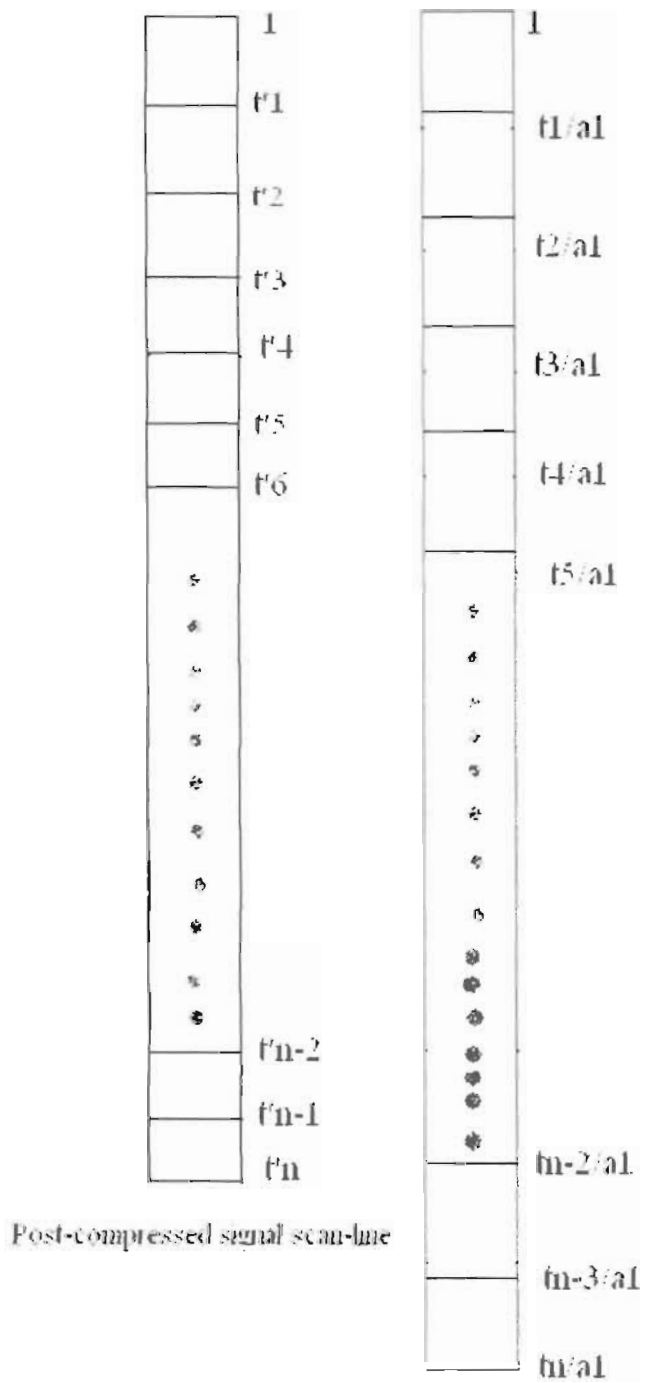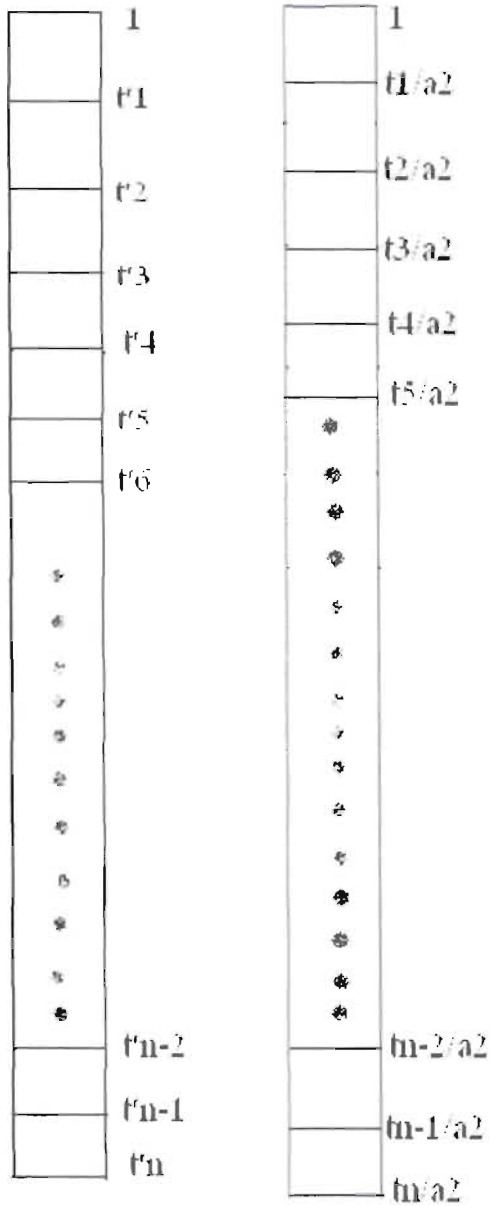
Post-compressed signal scan line	Pre-compressed signal scan-line
1	1
t'1	t1
t'2	t2
t'3	t3
t'4	t4
t'5	t6
t'6	
t'n-2	tn-2
t'n-1	tn-1
t'n	tn

Figure4.12: One scan-line of pre-compressed signal and post-compressed signal.

Post-compressed signal scan-line

Pre-compressed signal scan-line

Figure4.13: Entire scan-line of pre-compressed signal is compressed by compression factor 'a$_1$' and post-compressed signal is artificially uncompressed.

Post-compressed signal scan-line

Pre-compressed signal scan-line

Figure4.14: Entire scan-line of pre-compressed signal is compressed by compression factor 'a$_2$' and post-compressed signal is artificially uncompressed.

We extract the first block of pre-compressed signal from uncompressed scan-line and matching with the corresponding same size block of post-compressed signal using equation4.1 and find the matching index. Then we extract the first block of pre-compressed signal from 'a_1' compression scan-line and matching with the corresponding same size block of post-compressed signal using equation4.2 also find the matching index. In this way we extract the first block of pre-compressed signal from 'a_2', 'a_3', 'a_4', ..., 'a_i' sequentially. In all cases we observed the best matching position from maximum matching index using equation4.4. When best matching position is obtain then second block of post-compressed signal is start from that position and matching with the corresponding same size block of pre-compressed signal using equation4.5. This process is continuous for compression factor 'a_2', 'a_3', 'a_4', ..., 'a_i' sequentially. In all cases we obtain the best matching position from maximum matching index. In this way we extract third, fourth, fifth, ..., nth block of all scan-line sequentially and done same job.

4.2.4 Result of frame compression technique

We obtain the amount of compression (a_i) from the maximum matching index for all blocks of all scan-lines. The amount of compression for all blocks of one scan-line is as shown in figure4.15 and figure4.17 for real ultrasound data and synthetic data respectively. If hard tissue or cancer tissue is present then amount of compression factor is smaller compare to normal or soft tissues compression factor. Because, for hard tissue maximum matching index is obtain by small amount of compression factor. But for normal or soft tissue amount of compression is larger compare to hard tissue also shown in figure4.15. Finally display the B-mode elasticity image as shown in figure4.16 and figure4.18 for real ultrasound data and synthetic data respectively. B-mode elasticity image contain the amount of compression for all blocks of all scan-lines.
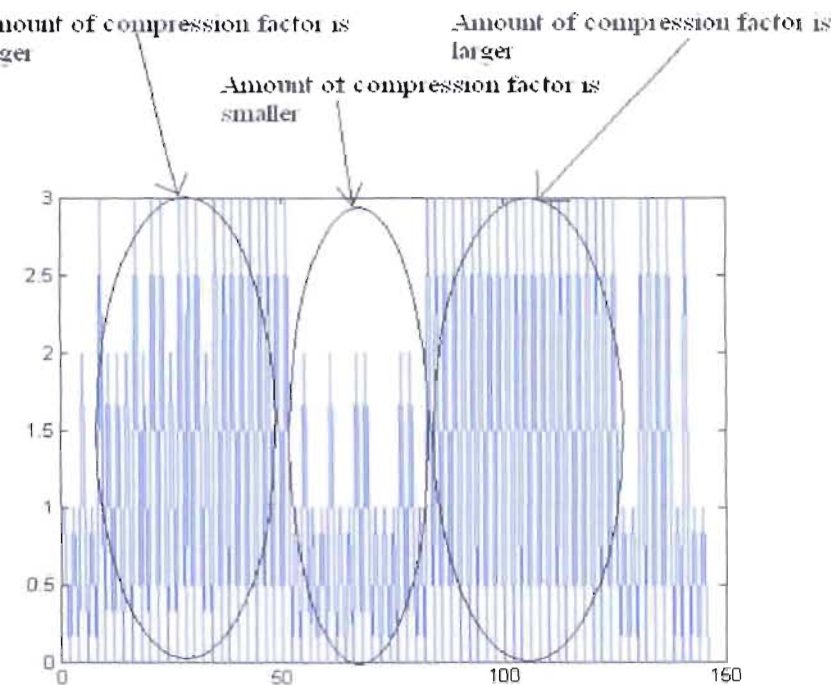
Figure4.15: Amount of compression for all blocks of one scan-line for real ultrasound data using ...me compression technique.
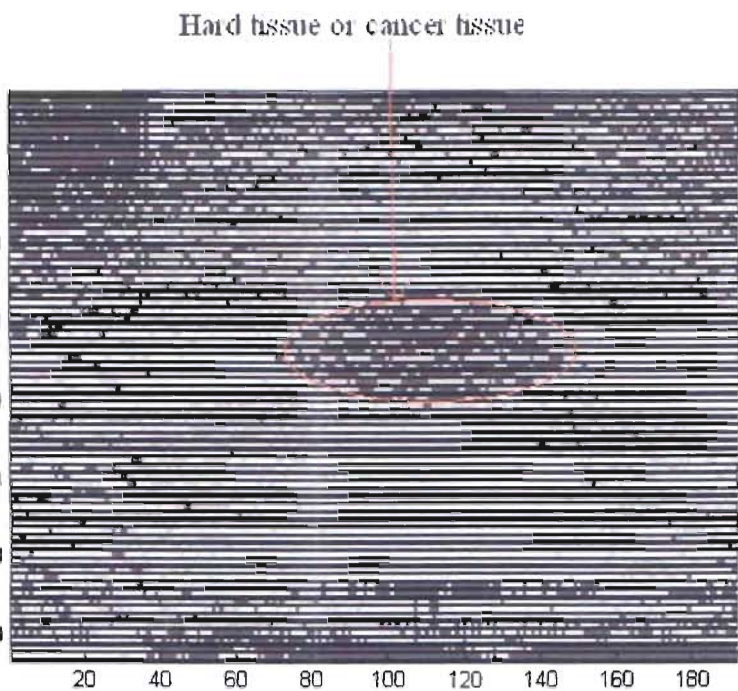

Figure4.16: B-mode elasticity image for real ultrasound data using frame compression ...chnique.
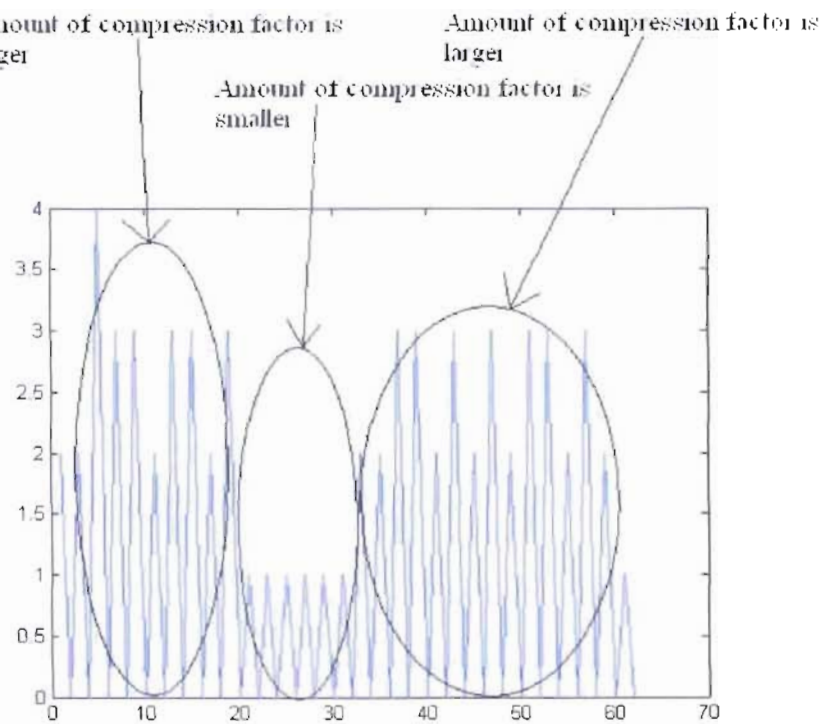
41

Figure4.17: Amount of compression for all blocks of one scan-line for synthetic data using frame compression technique.
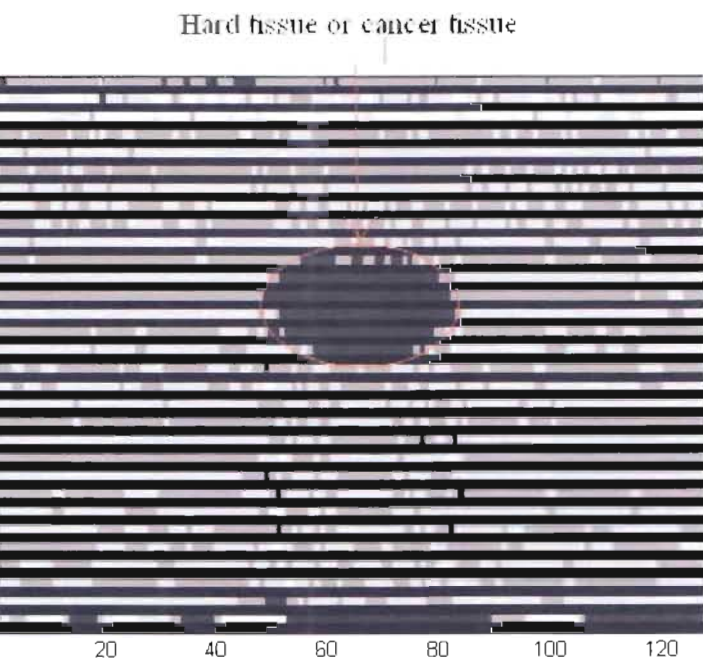

Figure4.18: B-mode elasticity image for synthetic data using frame compression technique.

-mode elasticity image is an amount of compression for all blocks of all scan-line. B-mode lasticity image detect the hard tissue or cancer tissue surrounding the normal tissue. In other vord B-mode elasticity image differentiate between normal tissue and hard tissue. The cancer issue is indicated by red color circle in B-mode elasticity image (shown in figure4.16 and igure4.18). But in these B-mode images several noise are occurs in cancer tissue and urrounding normal tissue. And these images are looking like so clumsy (shown in figure4.16 nd figure4.18). There are unwanted peak is occurs in amount of compression image of one can-line (shown in figure4.15 and figure4.17). Reason is that taking matching position at liscrete points. To overcome this situation we introduce several approaches. At first, we choose Linear Interpolation' technique.

.3 Linear interpolation

_inear interpolation is a method of curve fitting using linear polynomials. In this approach natching position can be found discrete position as well as continuous position. Linear nterpolation technique is described bellow:-

Ne are applying 'Linear Interpolation' technique for improving the quality of image. For :ompression a block or entire scan line we use four compression factors. They are zero, a_1, a_2, a_3, $_4$ respectively. If compression factor is zero or a_4 then linear interpolation is not required. Linear nterpolation actually fit a curve taking three points. When curve fitting is complete, we get the ictual peak. Actual peak may occur in the continuous point as well as discrete point. For the ollowing figure, the position can be calculated using a formula that is
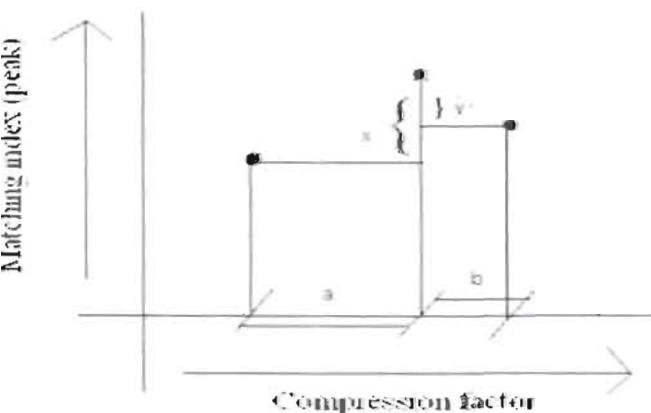

Figure4.19: Calculation of peak (Pixel) taking three points using 'Linear Interpolation' echnique.

43

rmula: $\dfrac{a}{b}=\dfrac{x}{y}$ this can formulate as $\dfrac{a}{a+b}=\dfrac{x}{x+y}$

$a=\dfrac{x\cdot(a+b)}{x\cdot y}$ .... (4.7)

llowing figures are shown that where peak may found when 'Linear Interpolation' technique applied

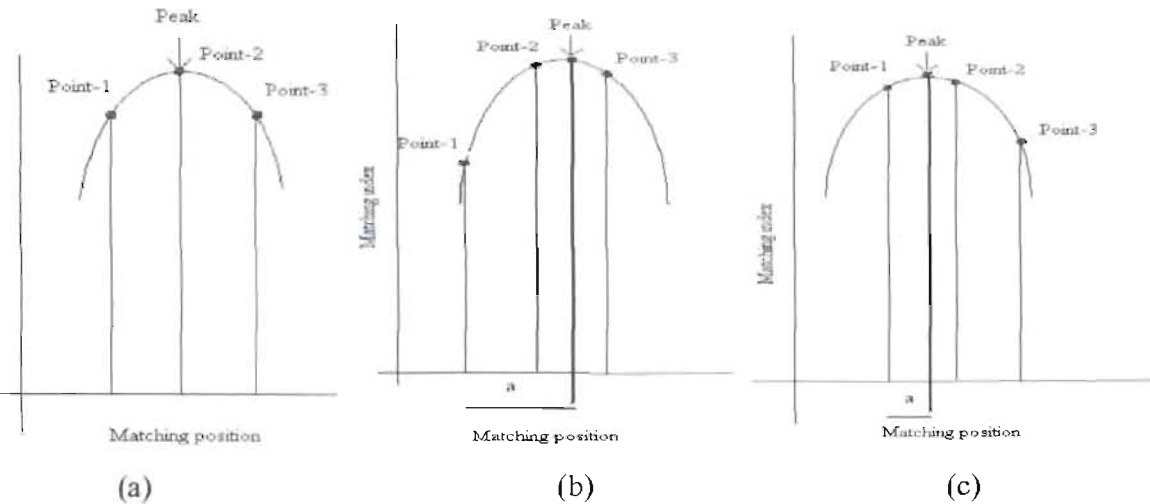(a)   (b)   (c)

gure4.20: (a) Peak occurs at mid position.

(b)Peak(point-x) occurs in between point-2 and point-3

(c)Peak(point-x) occurs in between point-1 and point-2

above figure4.20(a) shown that when matching value at point-1 and point-3 are same and int-2 in between them then peak or maximum matching value occurs at point-2 position. This sitin is best matching position. If matching value at point-1 and point-3 are not same then aximum matching does not occurs in the point-2. Maximum matching value is occurs in tween point-2 and point-3 if matching value at point-3 is greater then matching value at point- Then maximum matching position or best matching position observed by equation4.7 plus sition at point-1 as shown in figure4.20(b). And maximum matching value is occurs in tween point-1 and point-2 if matching value at point-1 is greater then matching value at point- Then maximum matching position or best matching position observed by equation4.7 plus sition at point-1 as shown in figure4.20(c). Finally we display the maximum matching value

44

all scan line. This is B-mode elasticity image as shown in figure4.22 and figure4.24. After ... en linear interpolation best matching position found at continuous position as well as discrete ...sion as shown in figure4.21 and figure4.23. The quality of the B-mode elasticity image is ...ter the previous B-mode image for both real ulrasound data and synthetic data.
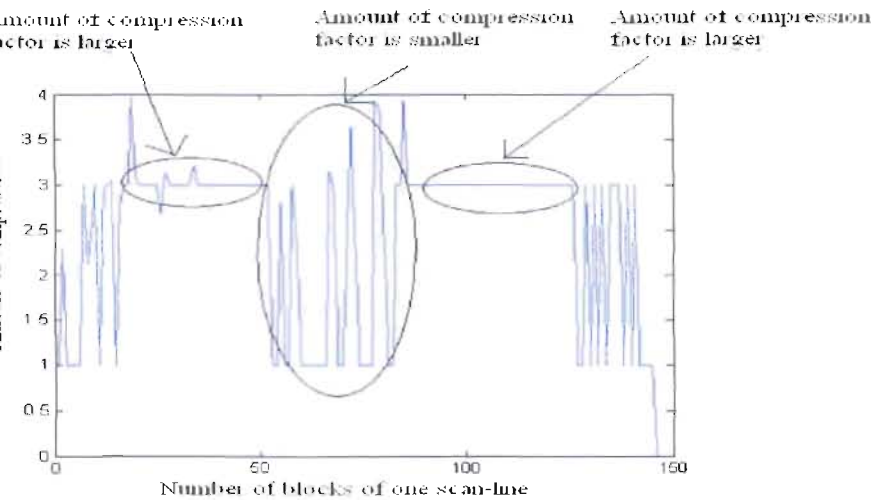
.1 Result after using linear interpolation

...gure4.21: Amount of compression for all blocks of one scan-line for real ultrasound data after ...ng the linear interpolation
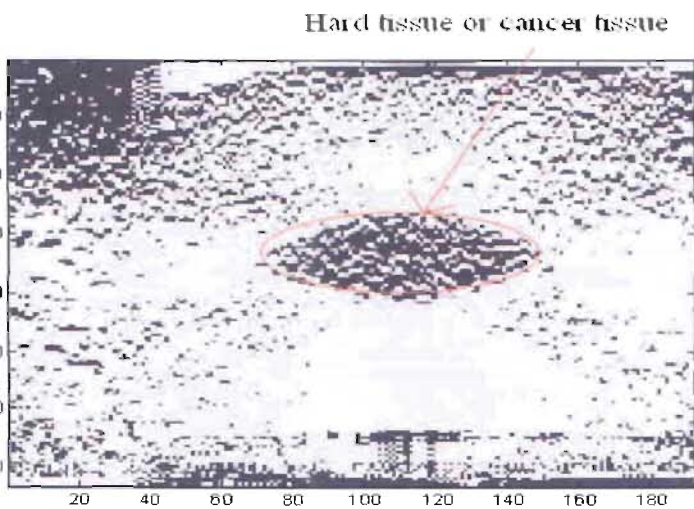

...gure4.22: B-mode elasticity image for real ultrasound data after using linear interpolation.
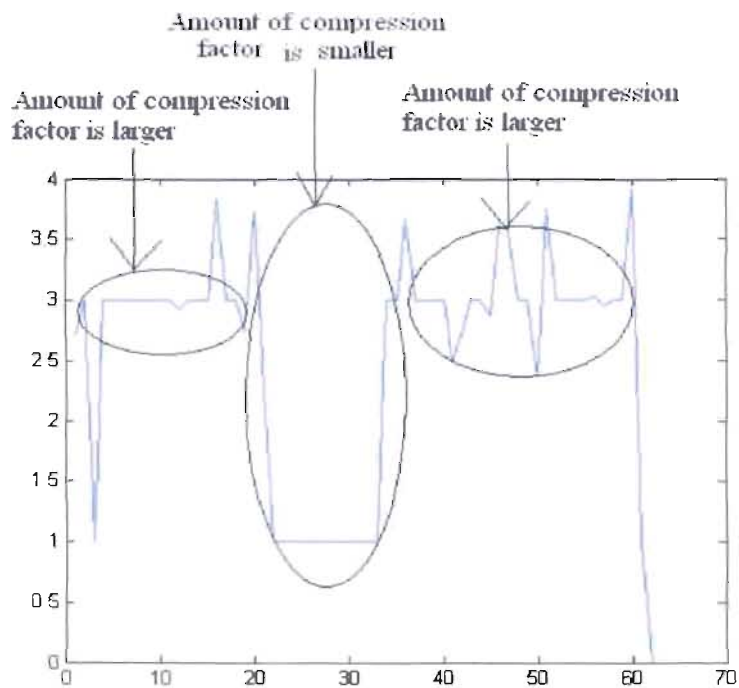
Figure4.23: Amount of compression for all blocks of one scan-line for synthetic data after using linear interpolation.
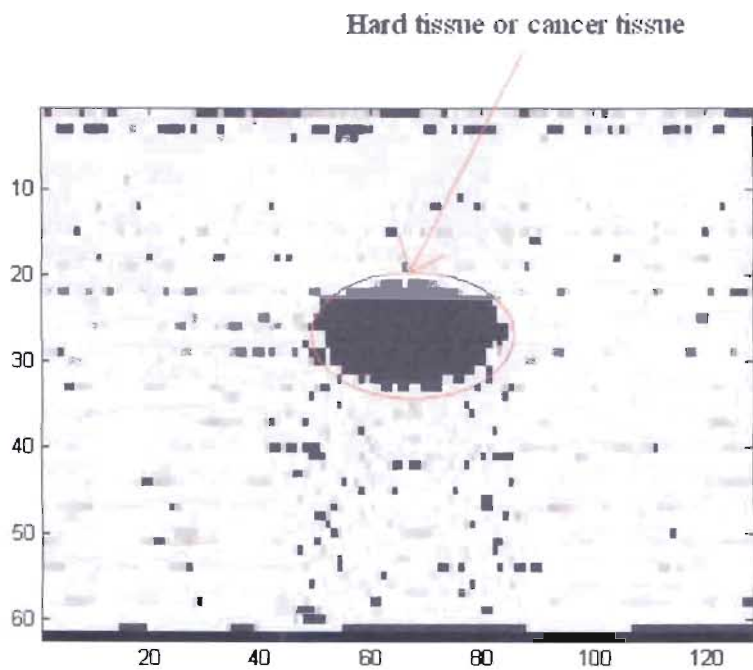

Figure4.24: B-mode elasticity image for ultrasound data after using linear interpolation.

After observing above figures, we can say that B-mode image quality is improved much from previous and matching positions are found at continuous points. After taking the linear interpolation discrete mode is also present inside and outside the hard tissue as shown B-mode elasticity image for real ultrasound data and synthetic data. To overcome this problem, we finally use 'Median Filter'.

.4 Median filter

The purpose of using median filter is outside region of hard tissue, there is a mixture of pixels of white and black colors. But the numbers of pixels of white color is very more than the pixels of black colors. Again within hard tissue region, number of pixels of black colors is more than pixels of white colors. Generally soft tissue is seen by us as white color and hard tissue as black color as shown in figure4.22 and 4.24. Use of median filter is another approach for getting better quality of B-mode elasticity image. Median filter takes the all values from the m*n then it sorting the values in ascending order. Finally extract the middle value from these values and paste into first row and first column in m*n matrix. For median [2, 2] filter it takes all values from 2*2 matrix within m×n matrix. Then sorting these values in ascending order. Next obtain the average value of two middle values and paste the value into the first row and first column in m*n matrix. The working principle of median [2, 2] filter is given bellow.

$$M = \begin{matrix} 0.5341 & 0.8385 & 0.7027 \\ 0.7271 & 0.5681 & 0.5466 \\ 0.3093 & 0.3704 & 0.4449 \end{matrix}$$

After using median filter the result is

$$M = \begin{matrix} 0.6476 & 0.6354 & 0.2733 \\ 0.4692 & 0.4957 & 0.2224 \\ 0.1546 & 0.1852 & 0 \end{matrix}$$

In this way same job is occurring within an m×n matrix.
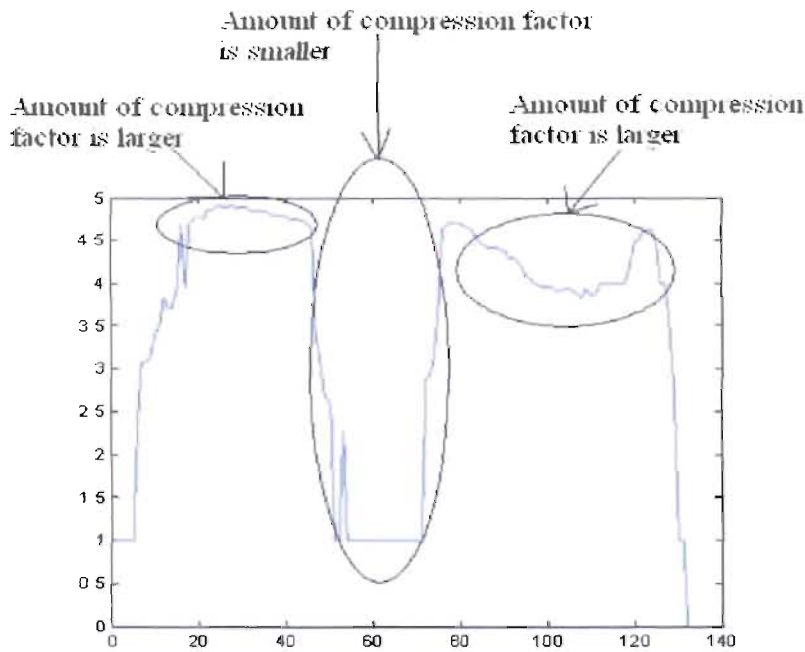
4.4.1 Result after using median filter

Figure4.25: Amount of compression for all blocks of one scan-line for real ultrasound data after using linear interpolation and median filter.
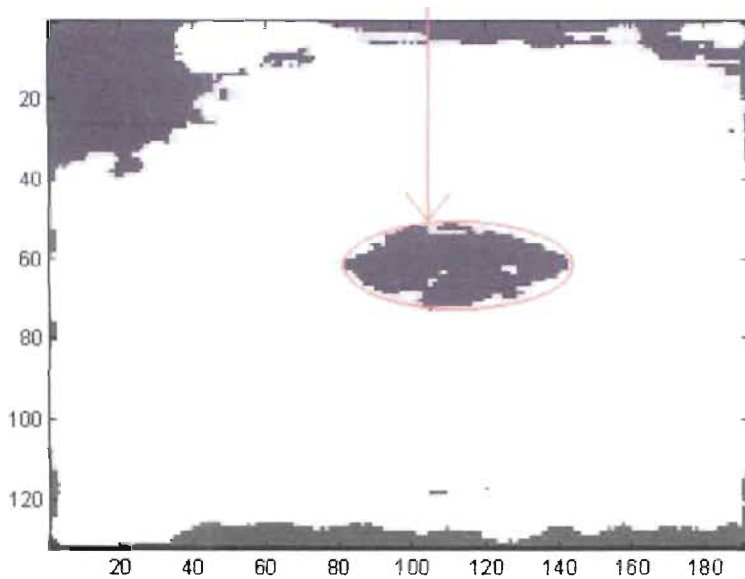

Figure4.26: B-mode elasticity image for real ultrasound data after using linear interpolation and median filter.
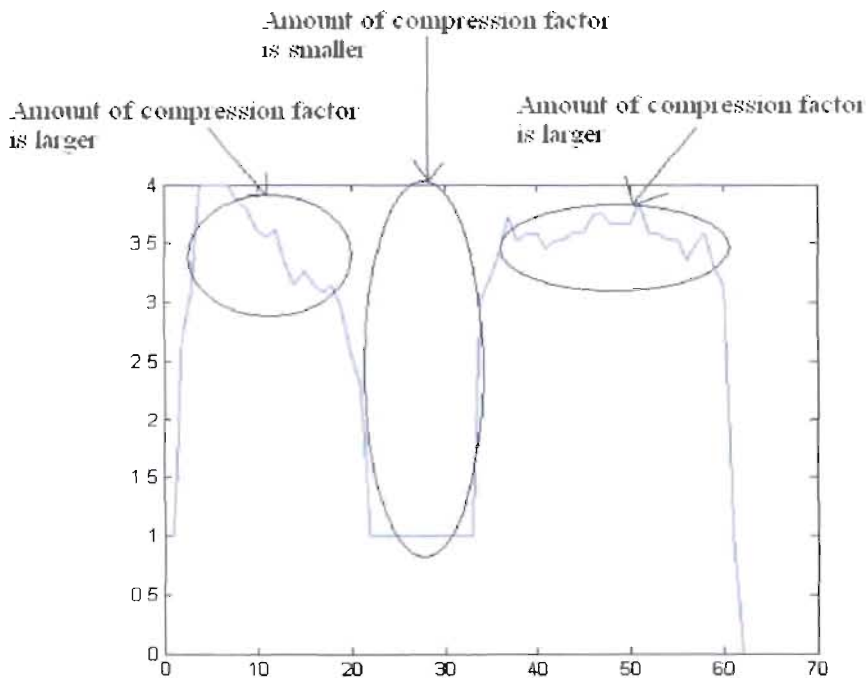
Figure4.27: Amount of compression for all blocks of one scan-line for synthetic data after using linear interpolation and median filter.
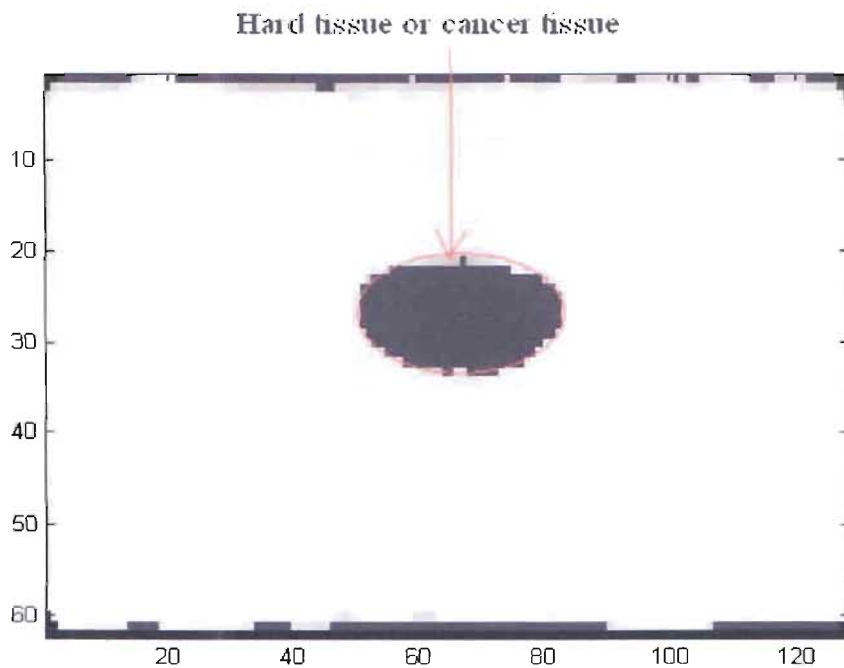

Figure4.28: B-mode elasticity image for synthetic data after using linear interpolation and median filter.

The amount of compression factor for all of one scan line is better than the previous amount of compression factor. Because using linear interpolation and median filter we get continuous and discrete values for amount of compression data. From figure4.25 and figure4.27 shown that amount of compression curve is smooth and unwanted peak is reduced. In B-mode elasticity image, it is clear to seen differentiate between hard tissue or cancer tissue surrounded by soft tissue. And B-mode elasticity image is so smooth and discrete point is removed. From figure4.26 and figure4.28 shown that hard tissue or cancer tissue is represent as dark and soft tissue is represent as bright. Inside of red circle indicate the cancer tissue or hard tissue and outside of red circle indicate the normal tissue.

4.5 comparisons

In real ultrasound data for compression factor 3 and window size or block size 128 we observed the best quality B-mode elasticity image. And in synthetic data for compression factor 3 window size 256 we observed the best quality B-mode elasticity image.
We fixed the compression factor and vary the window length for real ultrasound data and synthetic data:

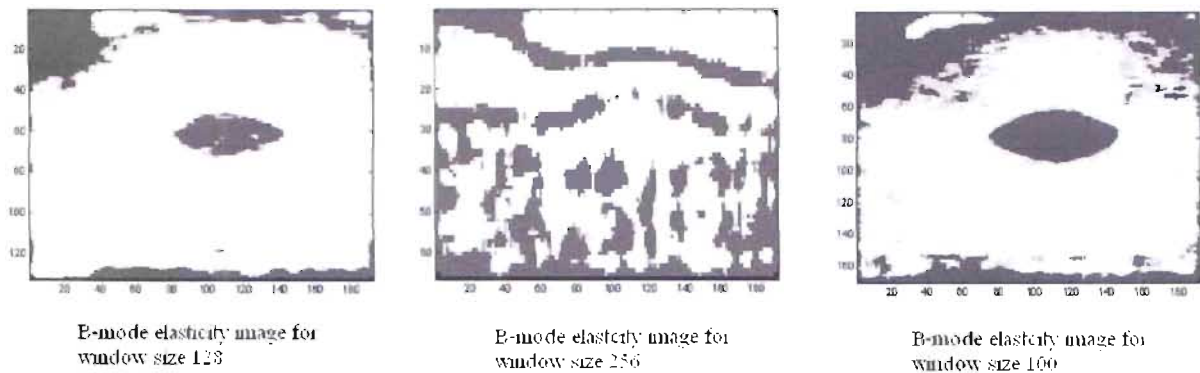B-mode elasticity image for window size 128   B-mode elasticity image for window size 256   B-mode elasticity image for window size 100

Figure4.29: In real ultrasound data B-mode elasticity image for compression factor 3 and variable window size.

50

B-mode elasticity image for
window size 128

B-mode elasticity image for
window size 200
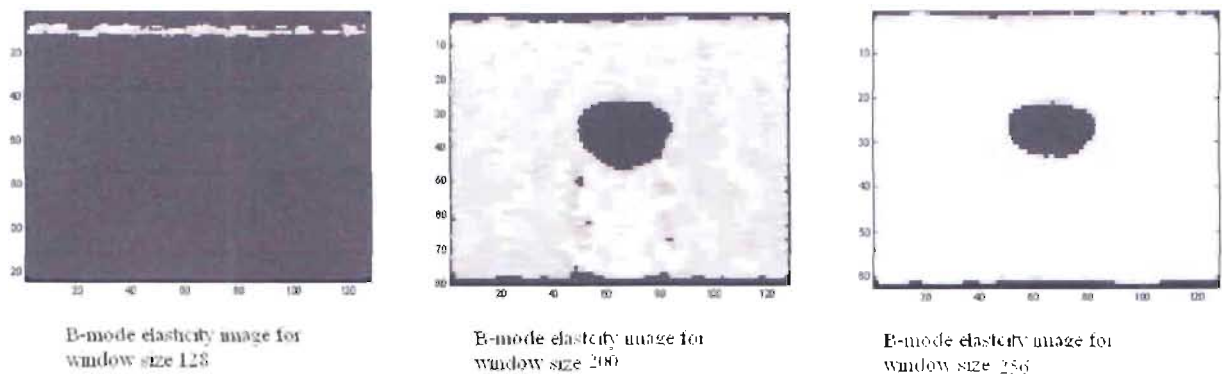
B-mode elasticity image for
window size 256

Figure4.30: In synthetic data B-mode elasticity image for compression factor 3 and variable window size.

In real ultrasound data for window size 128 we get the best B-mode elasticity image as shown in figure4.29. And in synthetic data for window size 256 we get the best b-mode elasticity image as shown in figure4.30.

Then we fixed the window size and vary the compression factor for real ultrasound data and synthetic data:
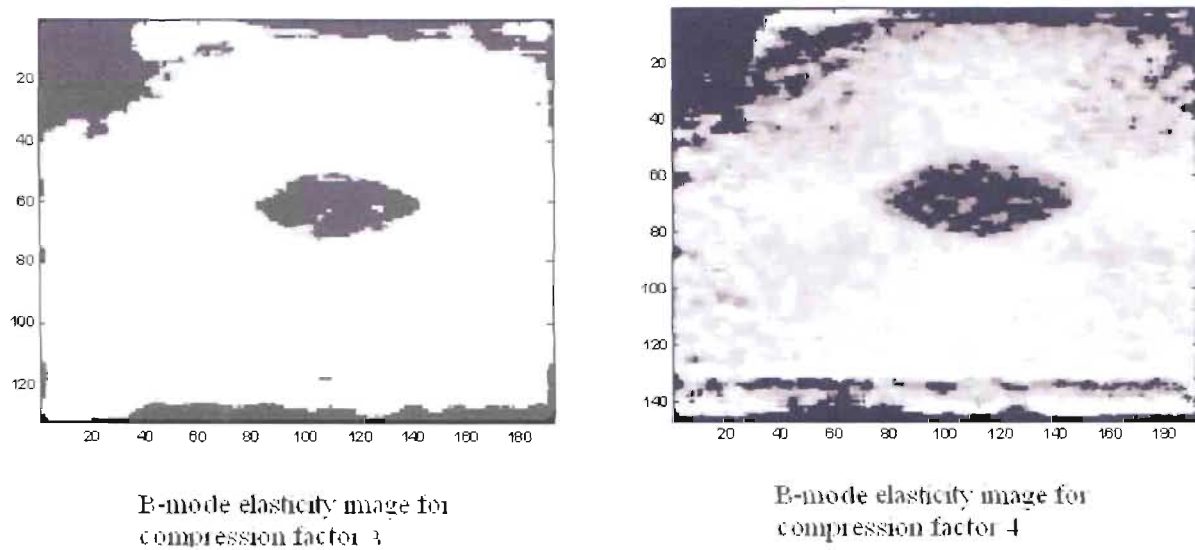

B-mode elasticity image for
compression factor 3

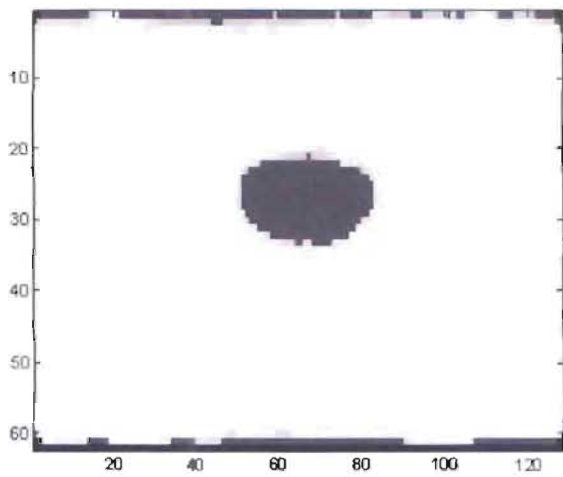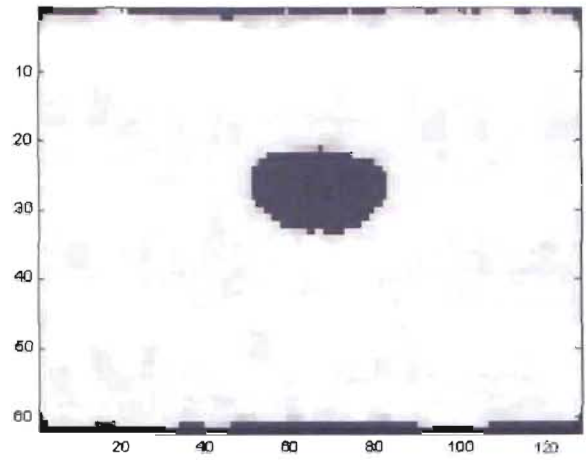B-mode elasticity image for
compression factor 4

Figure4.31: In real ultrasound data B-mode elasticity image for window size 128 and variable compression factor.

B-mode elasticity image for
compression factor 3

B-mode elasticity image for
compression factor 4

Figure4.32: In synthetic data B-mode elasticity image for window size 256 and variable compression factor.

Chapter 5

Conclusion

5.1 Summary

Ultrasound imaging is a real-time and relatively inexpensive imaging technique that is used in the purpose of clinical practice such as for non-invasive imaging and diagnosis of various tissue abnormalities. Changes in tissue elasticity are generally correlated with its pathological state. But change in mechanical properties of cancer tissues can't be detected by normal ultrasound imaging. Correlation based methods for ultrasound imaging are simpler, cheaper but posses their own limitations Research shows that, normal correlation can't detect cancer tissues exactly because this technique gives false peak of the signal. Therefore, people are trying to invent new ultrasound imaging techniques to detect cancer. For this purpose we worked on, ultrasound based electricity imaging technique technology which made the process of cancer detection feasible technically and economically. In our work we construct an elasticity image from the radio frequency ultrasound signals acquired before and after applying a physical pressure in the region of interest. From our thesis we observed that, normal B-mode imaging real ultrasound RF data and synthetic ultrasound data cannot detect the cancer or hard tissue surrounding by normal tissue. So, block and frame compression techniques are done in this thesis to improve the strain image. But the research shows, in real time the enhancement does not reach to the benchmark. On the other hand, block and frame compression techniques based strain image provide significantly informative image for the cancer identification. The signal processing task for generating a strain image is estimation of local compression throughout the scan region. The performance comparison between these two techniques is quite similar but computational time is a factor in the algorithm between these two techniques. Frame compression technique provides a faster algorithm than block compression technique. Finally constructed strain image is smooth by using a median filter.

5.2 Future Works

Correlation based methods for ultrasound imaging are simpler, cheaper but posses their own limitations. False peak of the signal occurs in this method which is an obstacle to detect cancer. In our work, this obstacle have been removed by using block and frame compression techniques which gives significantly informative strain image for identification of cancer tissues. But in our work we can't develop any algorithm for window size and compression factor for identification of cancer. So, algorithm development for window size as well as compression factor can be another prospective work for our developed techniques where efforts should be given. The relation between tissues elasticity and pathological classification can be a future arena of research. Then it will be possible to discriminate between benign and malignant tumors. The identification of strain image texture can be another field of work where efforts should be given. In addition, it is expected that in future, tissues elasticity imaging technology will be more sophisticated leading to the three dimensional strain image estimation as well as the quantitative study of elasticity images for different stages of diseases will take place. Finally, the remedy of consequences of correlation based strain imaging can be a prospective fields as this technique still its appeals.

References

1. A. Jemal, R.C. Tiwari, T. Murray, A. Ghafoor, A. Samels, E. Ward, E.J. Feuer, M.J. Thun: Cancer Statistics 2004, CA - A cancer journal for clinicians, 54(1): 8-29, 2004.

2. http://www.greatdreams.com/cancer-cure.htm

3. 12 W.A.D Anderson. Pathology. CW Mosby Co., St. Louis, 1953.

4. S.Y. Emelianov, S.R Aglyamov, J. Shah, S. Sethuraman, W.G. Scott, R. Schmitt, M. Motamedi, A. Karpiouk, A. Oraevsky, 'Combined ultrasound, optoacoustic and elasticity imaging'

5. Lerner RM, Parker KJ: Sonoelasiticity images, ultrasonic tissue characterization and echo graphic imaging. In Proceedings of the 7′European Communities Workshop. Nijmegen, The Netherlands, 1987.

6. Gao L, Alam SK, Lerner RM, Parker KJ; Sonoelasticity imaging: theory and experimental verification. J Acoust SOC Am, in press.

7. L Sandrin, S Catheline, M Tanter, X Hennequin, and M Fink. Time-resolved pulsed elastography with ultrafast ultrasonic imaging. Ultrasonic Imaging, 21(4):259–272, October 1999. PMID: 10801211.

8. Ophir J, Cespedes I, Ponnekanti H, Yazdi Y, Li X: Elastography: a quantitative method for imaging the elasticity of biological tissues. Ultra-SonicImaging 13:111-134, 1991.

9. O'Donnell M, Skovoroda AR, Shapo BM, and Emelianov SY: Internal displacement and strain imaging using ultrasonic speckle tracking. IEEE Trans Ultrasonics Ferroelect Freq Contr41: 314-325, 1994.

10. Skovoroda AR, Emelianov SY, Lubinski MA, Sarvazyan AP, O'Donnell M: Theoretical analysis and verification of ultrasound displacement and strain imaging. IEEE Trans Ultrasonics Ferroelec Freq Contr 41:302-313, 1994.

11. Walker WF, Friemel BH, Laurence NB, Trahey GE: Real-time imaging of tissue vibration using a two-dimensional speckle tracking system. Proceedings 1993 IEEE Ultrasonics Symposium. 873-877, 1993.

12. Averikiou, M. A., Tissue Harmonic Imaging, Proceedings of the IEEE Ultrasonics Symposium, pp.1561-1566, 2000.

13. Thomenius, Kai E., Evolution of Ultrasound Beamformers, Proceedings of the IEEE Ultrasonics Symposium, pp.1615-1922, 1996.

14. Feller-Kopman D: Ultrasound-guided thoracentesis. Chest 2006; 129:1709-1714